Current Research (2024) Newfoundland and Labrador Department of Industry, Energy and Technology
Geological Survey, Report 24-1, pages 155-180

NEW U–Pb SHRIMP AGE CONSTRAINTS ON THE GEODYNAMIC EVOLUTION OF THE HOPEDALE BLOCK, LABRADOR: IMPLICATIONS FOR THE ASSEMBLY OF THE NORTH ATLANTIC CRATON

A.M. Hinchey, N. Rayner[1], D. Diekrup, H.A.I. Sandeman[2] and D. Mendoza Marin
Regional Geology Section
[1]Geological Survey of Canada, 601 Booth Street, Ottawa, Ontario K1A 0E8
[2]Mineral Deposits Section

ABSTRACT

In Labrador, the North Atlantic Craton comprises the northern Saglek and southern Hopedale blocks. The Archean history of the Hopedale Block is punctuated by several plutonic, volcanic and metamorphic events. New SHRIMP U–Pb zircon geochronological data further refine the Archean tectonomagmatic evolution of the region. The oldest dated event is the formation of the protoliths of the Maggo Gneiss at ca. *3262–3245 Ma. Between* ca. *3141 and 3105 Ma, the area experienced a magmatic event that included at least three plutonic pulses and the deposition of the Hunt River Group. Based on crosscutting relationships and new geochronological data, a newly identified package of volcanosedimentary rocks older than* ca. *3124 Ma is identified, and possibly another, older than* ca. *3262 Ma. Between* ca. *3032 and 2979 Ma, events included the intrusion of plutonic suites and the deposition of the Florence Lake Group. These rocks were collectively intruded by the* ca. *2892–2832 Ma Kanairiktok Intrusive Suite. This was followed by a plutonic event at* ca. *2720–2710 Ma, and the youngest Archean event is the emplacement of the* ca. *2578–2545 Ma Aucoin Plutonic suite. The oldest evidence of metamorphism is cryptic at* ca. *2961–2953 Ma, preserved as zircon overgrowths on two samples. Most of the metaplutonic suites in the block preserve evidence of widespread metamorphism at* ca. *2846–2796 Ma and* ca. *2732–2700 Ma (as zircon overgrowths and titanite growth). The* ca. *2846–2796 Ma metamorphic events are geographically widespread and synchronous, in part, with the intrusion of the Kanairiktok Intrusive Suite. The Kanairiktok Intrusive Suite is hypothesized to represent a continental magmatic-arc that formed during the initiation of plate tectonics in the region. Based on widespread occurrence in both blocks, the* ca. *2732–2700 Ma metamorphic event likely corresponds to the collision between the Saglek and Hopedale blocks. One outcrop preserves evidence of a* ca. *2554–2542 Ma metamorphic event (as zircon overgrowths), and as this event is only documented locally, it may be restricted to the western Hopedale Block. No evidence of the previously proposed Hopedalian metamorphic event is observed and little evidence for the Fiordian event.*

INTRODUCTION

North-central Labrador is geologically complex and located at the junction of five tectonic domains (Figure 1). These include the Hopedale Block, Saglek Block, Core Zone, Torngat Orogen and Makkovik Province. The Hopedale and Saglek blocks form the Nain Province, part of the North Atlantic Craton (NAC), which extends through Greenland to northwest Scotland (Bridgewater *et al.*, 1973). The blocks represent two Archean crustal fragments that are inferred to have been juxtaposed along an ill-defined, north–northeast-trending high-strain zone as late as *ca.* 2560 Ma, based on sparse metamorphic and granitoid ages (Connelly and Ryan, 1996; Wasteneys *et al.*, 1996). The NAC is separated from the Core Zone by the *ca.* 1.89–1.85 Ga Torngat Orogen, a zone of intense transpression and high-grade metamorphism affecting the Tasiuyak Complex, the Lac Lomier Complex, and the eastern edge of the Core Zone (Figure 1; Wardle *et al.*, 2002; Godet *et al.*, 2021). To the south, the NAC is bounded by the Makkovik Province, a zone of Paleoproterozoic crustal reactivation and terrane accretion (Ketchum *et al.*, 2002; Hinchey *et al.*, 2020, 2023a). The area was subsequently intruded by voluminous anorthosite–mangerite–charnockite–granite (AMCG) plutonism (Nain Plutonic Suite (NPS) and Harp Lake Intrusive Suite (HLIS)) and peralkaline magmatism (Flowers River Igneous Suite (FRIS); Figure 1).

This report highlights new geochronological constraints on the evolution of the Hopedale Block and provides an

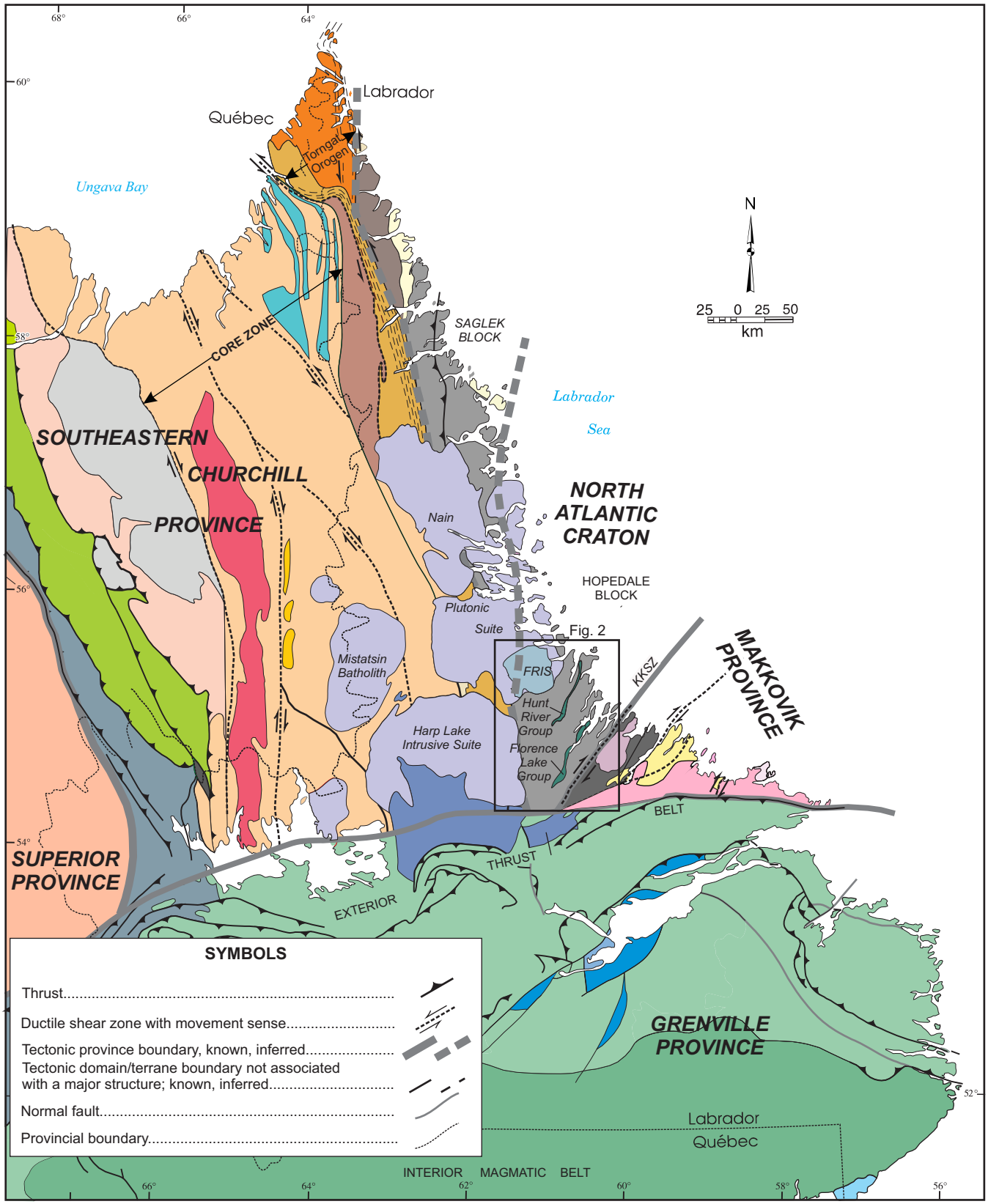

Figure 1. *Simplified geological map of eastern Québec and Labrador (modified after Hinchey* et al.*, 2023b). KKSZ= Kanairiktok Shear Zone; FRIS=Flowers River Igneous Suite. The location of Figure 2 is outlined.*

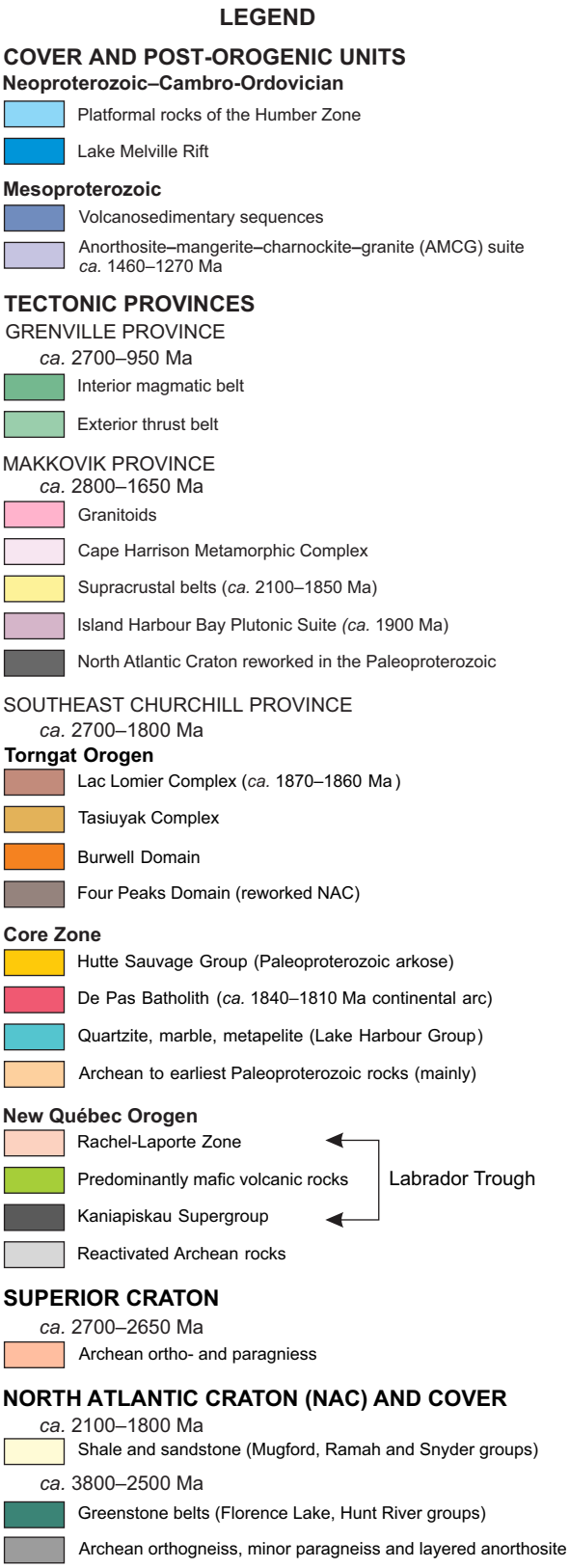

Figure 1. *Legend*

updated tectonostratigraphic column for the Archean history of the region. This research is part of a joint project between the Geological Survey of Canada (Geoscience for Minerals and Energy – GEMII and GEM-GeoNorth), the Geological Survey of Newfoundland and Labrador, and the Nunatsiavut Government. Geochronological data previously released as part of this project (Rayner, 2022), as well as historical datasets (Loveridge *et al.*, 1987; Schiøtte *et al.*, 1989; Wasteneys *et al.*, 1996; James *et al.*, 2002) are integrated into a revised, geological framework.

HOPEDALE BLOCK GEOLOGY

Historically, the geology of the Hopedale Block has been described as composed of variably deformed and metamorphosed Archean orthogneisses grouped as the Maggo Gneiss. The gneiss was intruded by the Archean mafic Hopedale dykes after the poorly defined >3100 Ma Hopedalian high-grade metamorphic and penetrative deformation event (Korstgård and Ermanovics, 1985; James *et al.*, 2002). Two supracrustal (greenstone) belts were mapped in the region, the *ca.* 3105 Ma, amphibolite facies, Hunt River Group (HRG, sometimes referred to as the Hunt River belt or Hunt River greenstone belt), and the *ca.* 3003–2979 Ma, greenschist to amphibolite facies, Florence Lake Group (FLG, sometimes referred to as the Florence Lake belt or Florence Lake greenstone belt; Wasteneys *et al.*, 1996; James *et al.*, 2002). Numerous narrow lenses and rafts of dismembered volcanic, sedimentary, and ultramafic rocks are variably grouped as the Weekes Amphibolite or, if proximal to the Hunt River or Florence Lake groups, were incorporated with the adjacent group (Ermanovics, 1993). In early interpretations, the HRG rocks were considered the oldest in the region (Ermanovics, 1993; Wasteneys *et al.*, 1996). However, U–Pb geochronological studies have demonstrated that components of the Maggo Gneiss represent an older, although poorly defined (*ca.* 3300 to >3100 Ma; Loveridge *et al.*, 1987; James *et al.*, 2002) suite of basement rocks. Preliminary work suggested that the Weekes Amphibolite may be, in part, related to the HRG (Ermanovics, 1993) and this was supported by their similar lithochemistry and isotopic data (Sandeman *et al.*, 2023). The FLG was the youngest known volcanosedimentary rocks in the region at *ca.* 3003–2979 Ma (Wasteneys *et al.*, 1996; James *et al.*, 2002; Diekrup *et al.*, 2023).

Ermanovics (1980) indicated that from *ca.* 2960–2880 Ma, the Maggo Gneiss, Weekes Amphibolite, HRG and FLG were deformed and metamorphosed at greenschist- to amphibolite-facies during the Fiordian high-grade metamorphic and ductile deformation event. These rocks were then intruded by tonalite and granodiorite of the *ca.* 2883–2848 Ma Kanairiktok Intrusive Suite (KIS; Loveridge *et al.*, 1987; Rayner, 2022). This suite engulfs the older units and

was interpreted as being contemporaneous with the latter stages of, and locally postdating, the Fiordian event (Korstgård and Ermanovics, 1985; Ermanovics, 1993; James *et al.*, 2002). The driving mechanism of the Fiordian event is uncertain, but it is interpreted to have resulted in the strongly developed, northeast-trending structural fabric in the southeast part of the block (Ermanovics, 1980). The final Neoarchean event was the intrusion of the *ca.* 2567 Ma Aucoin Plutonic suite (Sandeman and McNicoll, 2015).

During the Mesoproterozoic, voluminous AMCG magmas intruded the region, and included the NPS and HLIS (Figure 1). The products of slightly younger, peralkaline volcanism and plutonism are preserved in the *ca.* 1272 Ma Flowers River Igneous Suite (Hill, 1991; Ducharme, 2018; Rayner, 2022). Abundant mafic dykes intruded the region between 2238 ± 6 Ma and 2216 ± 2 Ma (*i.e.*, Kikkertavak dykes) and 1273 ± 1 Ma (*i.e.*, Harp dykes; Cadman *et al.*, 1993, Sahin and Hamilton, 2019).

PETROGRAPHY AND U–Pb GEOCHRONOLOGY

ANALYTICAL METHODS

Thin Section Imagery

Polished thin sections were imaged using Energy Dispersive X-ray Spectroscopy-Scanning Electron Microscopy-Mineral Liberation Analysis (EDS-SEM-MLA) and an optical microscope. Analytical details are described in Feely *et al.* (2019). The MLA software provides a false-colour digital map of the mineral phases present within a rock thin section and it also yields mineral abundance data (as a function of the area percent of the analyzed thin section).

Geochronology

Zircon from each of the five samples reported herein was imaged by scanning electron microscope before U–Pb isotopic analysis using the sensitive high-resolution ion microprobe (SHRIMP). A summary of the sample locations and interpreted ages is presented in Table 1. Sample locations are illustrated in Figure 2. Field photographs of sample locations are presented in Plate 1. Analytical data are reported in Supplemental Data.

All samples were comminuted using electropulse disaggregation (at Overburden Drilling Management Inc.) followed by density separation using the Wilfley table and heavy liquids, from which zircon separate was isolated by hand panning the heavy minerals. For SHRIMP analysis, selected grains were cast in epoxy mounts IP1995, 1004, 1016 and 1017. The minerals were exposed through polishing with a diamond compound, and internal features were characterized in back-scattered electron (BSE) and cathodoluminescence (CL) modes utilizing a TESCAN Mira3 scanning electron microscope. Mount surfaces were evaporatively coated with 10 nm of high-purity Au.

SHRIMP analytical procedures followed those described by Stern (1997). Fragments of primary zircon reference material (RM) 6266 ($^{206}Pb/^{238}U$ age = 559 ± 0.2 Ma, Stern and Amelin, 2003) and secondary zircon RM 1242 ($^{207}Pb/^{206}Pb$ age = 2679.7 ± 0.2 Ma, Davis *et al.*, 2019) were analyzed on the same mount and under the same conditions as the unknowns. Analyses were conducted using an O− primary beam, with a 20 μm diameter spot with a beam current between 4–10 nA. The count rates of the isotopes of U, Th and Pb as well as Hf and Yb for zircon were sequentially measured over six scans with a single electron multiplier. Off-line data processing was accomplished using either Squid2.5 (Ludwig, 2009) or Squid3 (Bodorkos *et al.*, 2020) software. Decay constants used follow the recommendations of Steiger and Jäger (1977). The 1σ external errors of $^{206}Pb/^{238}U$ ratios reported in the data table incorporate a ±0.8–0.85% uncertainty in calibrating the primary RM (Stern and Amelin, 2003). Analyses of a secondary zircon RM 1242 were interspersed between the sample analyses to assess the requirement of an isotopic mass fractionation correction for the $^{207}Pb/^{206}Pb$ age. Details of the analytical session (mount/session number, spot size, primary beam intensity) are recorded in the footnotes of the data table as is the measured weighted mean age for the secondary RM for that session and whether a mass fraction correction was applied. Common Pb correction utilized the Pb composition of the surface blank (Stern, 1997). Isoplot v. 4.15 (Ludwig, 2012) was used to generate concordia plots and calculate weighted means. The error ellipses on the concordia diagrams, and the weighted mean errors in the text and Table 1 are reported at 95% confidence unless otherwise noted. Uncertainties reported in the Supplemental Data are given at the 1σ confidence interval.

RESULTS

Metasedimentary Unit: Psammite (19AH004A; GSC Lab Number 12686)

This sample was collected from an outcrop located 3.5 km south-southeast of the community of Hopedale (Figure 2). The sample is from a white-weathering, fine-grained, foliated and recrystallized psammite (Plates 1A and 2A, B). The sample preserves amphibolite-facies metamorphism. The unit is several metres thick and occurs interlayered with

Table 1. Summary of U–Pb data for the Hopedale Block. Reported ages are from zircon grains except where indicated *i.e.*, t=titanite. Superscript numbers following the reported ages correspond to Figure 4. Latitude and longitude WGS84 datum

Station	Rock type	Group/Suite/Event	Crystallization age	Detrital (max. dep. age)	Metamorphic age	Latitude	Longitude	Reference
18AH011	tonalitic orthogneiss	Maggo Gneiss	3262±5 Ma[1]		2836±4 Ma[26] 2704±4 Ma(t)[39]	55.164560	-60.609010	Rayner, 2022
18AH015	tonalitic orthogneiss	Maggo Gneiss	3258±10 Ma[2]		2846±7 Ma[23]	55.610940	-60.402860	Rayner, 2022
DB83.47C	metapelite	unnamed		<3258±24 Ma[3]	2841±5 Ma[24]	55.594440	-60.398610	Schiøtte *et al.*, 1989
18CXAD0042	granodiorite orthogneiss	Maggo Gneiss	3247±12 Ma[4]		2833±9 Ma[27] *ca.* 2.7 Ga(t)[40]	55.586880	-60.395410	Rayner, 2022
Mg1 & MG2	tonalitic orthogneiss	Maggo Gneiss	3245±5 Ma[5]		2953±3 Ma[18] 2839±4 Ma(t)[25]	54.972220	-60.747220	James *et al.*, 2002
17CXA-D018	granodiorite	3.14–3.11 Ga event	3141±6 Ma[6]		2724±3 Ma[33]	55.459000	-60.218000	Rayner, 2022
17CXA-D017A1	tonalite	3.14–3.11 Ga event	3124±3 Ma[7]		2710±10 Ma[37]	55.803700	-60.486300	Rayner, 2022
HR2	tonalitic gneiss	3.14–3.11 Ga event	3107±3 Ma[8]		2961±2 Ma[17]	55.373060	-60.736390	James *et al.*, 2002
EE-78-189	orthogneiss	3.14–3.11 Ga event	3105+6/-9 Ma[9]			55.425090	-60.215720	Loveridge *et al.*, 1987
DJ-96-057	rhyolite	Hunt River Group	3105.2±2.5 Ma[10]			55.313890	-60.776390	James *et al.*, 2002
19AH004	psammite	unnamed		<3101±5 Ma[11]	2712 ± 4 Ma[37]	55.437007	-60.224353	This report
19AH001	granodiorite	3.03–2.96 Ga event	3032±4 Ma[12]		~2.7 Ga[40]	55.447445	-60.452388	This report
19AH002	monzogranite	3.03–2.96 Ga event	3011±4 Ma[13]		2831±11 Ma[29] 2717±8 Ma[35]	55.514601	-60.432587	This report
HW318-320	rhyolite	Florence Lake Group	3003±4 Ma[14]			54.898828	-60.853498	Wasteneys *et al.*, 1996A
DJ-95-325	rhyolite	Florence Lake Group	2990±2 Ma[15]			55.133330	-60.554170	James *et al.*, 2002
FL1	rhyolite	Florence Lake Group	2979±1 Ma[16]			54.799420	-60.845440	James *et al.* 2002
21AH041	quartz diorite	Kanairiktok Plutonic Suite	2892±4 Ma[19]		2807±19 Ma[30]	55.219790	-60.074679	This report
KP1	tonalite	Kanairiktok Plutonic Suite	2883±3 Ma[20]			54.775940	-60.838910	James *et al.*, 2002
EE-78-178	tonalite	Kanairiktok Plutonic Suite	2858+4/-3 Ma[21]		2796±2 Ma[31] [32]	55.291760	-60.097660	Loveridge *et al.*, 1987
18AH025	granodiorite	Kanairiktok Plutonic Suite	2848±7 Ma[22]		2732±8 Ma	55.376790	-61.590100	Rayner, 2022
18AH033	granodiorite	Kanairiktok Plutonic Suite	2832±6 Ma[28]			55.459600	-60.955400	Rayner, 2022
21AH105	granodiorite	2.73–2.70 Ga event	2720±5 Ma[34]		2554 ± 20 Ma[43]	55.369102	-61.501938	This report
17CXA-D018	granodiorite	Melt injection	2710±2 Ma[38]			55.459000	-60.218000	Rayner, 2022
HW216, 217	granite	Aucoin Plutonic Suite	2578±2 Ma[41]			55.327038	-61.467732	Wasteneys *et al.*, 1996A
AR96-01-65m	syenite	Aucoin Plutonic Suite	2567±4 Ma[42]			55.360376	-61.384208	Sandeman and McNicoll, 2015
HW238	granite	Aucoin Plutonic Suite	2554±4 Ma[44]			55.327038	-61.467732	Wasteneys *et al.*, 1996A

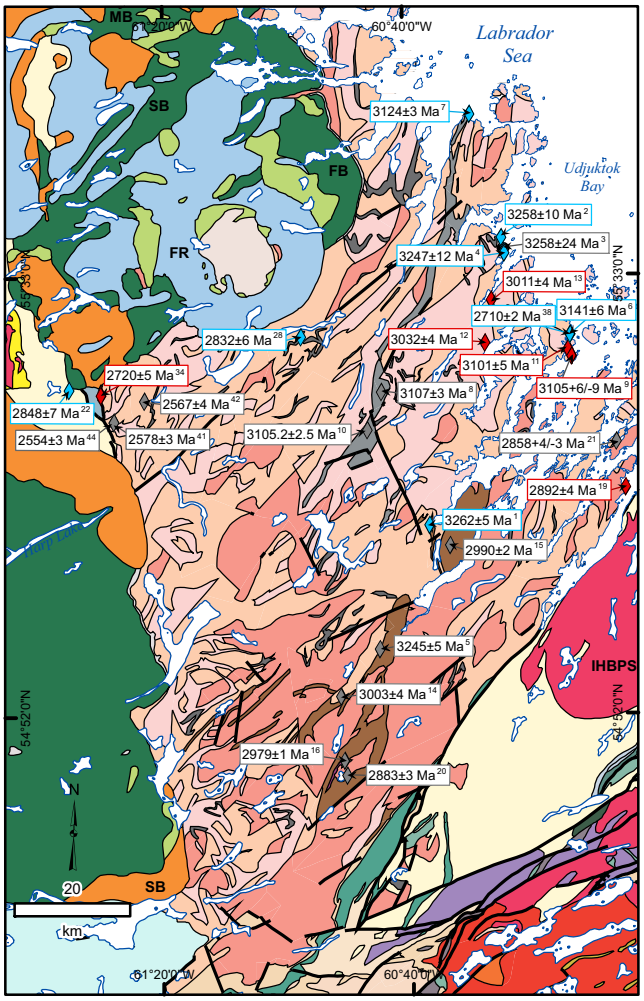

LEGEND

STRUCTURAL PROVINCES
MIDDLE PROTEROZOIC

Flowers River Igneous Suite (FRIS)
- Peralkaline volcanic rocks
- Peralkaline granite

Seal Lake Group

Granitoid Intrusions
- **Nain Plutonic Suite; granitoid rocks**
- Ferrodiorite, monzodiorite–diorite

Gabbroid Intrusions
- Anorthosite
- Gabbroic rocks

GRENVILLE PROVINCE AND ADJACENT AREAS
LOWER PROTEROZOIC

Bruce River Group

Trans-Labrador Batholith and Equivalents
- Granitoid rocks
- Crooked River granite

MAKKOVIK PROVINCE
LOWER PROTEROZOIC
- Diorite
- Granitoids *ca.* 1890–1800 Ma

Early Granitoid Plutons
- Granitoid to granodiorite

Moran Lake Group and Deformed Equivalents
- Joe Pond Formation

Post Hill Group (*ca.* <2013 Ma)
- Amphibolite and mafic metavolcanic rocks
- Metasedimentary schist and phyllite

Unassigned supracrustal rocks
- Schistose or phyllitic metasedimentary rocks
- Schistose metavolcanic rocks

ARCHEAN

Structurally Reworked Equivalents of Nain Province Rocks
- Granitoid metaplutonic rocks
- Granitoid gneisses; minor amphibolite

EASTERN CHURCHILL PROVINCE
LOWER PROTEROZOIC
- **Ingrid Group**
- Foliated to gneissic plutons
- **Tasiuyak Gneiss**

ARCHEAN
- Tonalitic–grandioritic, amphibiolite- to granulite-facies gneisses

NAIN PROVINCE
ARCHEAN
- Migmatite gneiss, in part from KIS and Maggo Gneiss
- Kanairiktok Intrusive Suite (KIS)

Florence Lake Group
- Mafic-volcanic and volcaniclastic rocks
- Serpentinized peridotite sills
- **Hunt River Group**
- **Weekes Amphibolite**
- **Maggo Gneiss**

SYMBOLS

Contact (defined, approximate)..... Fault.....

Figure 2. *Geological map of northcentral Labrador (simplified after Wardle, 1993). SL=Snegamook Lake Pluton; SB=Sango Bay pluton; FB=Flowers Bay pluton; MB=Merryfield Bay pluton; IHBPS=Island Harbour Bay Plutonic Suite; HLIS=Harp Lake Intrusive Suite; FR=Flowers River Igneous Suite. Locations of the U–Pb samples and details about their primary age constraint (crystallization or youngest detrital) are from Table 1 (identified by superscript numbers). Grey diamonds are from historical data, blue diamonds are from Rayner (2022) and red diamonds are from this study.*

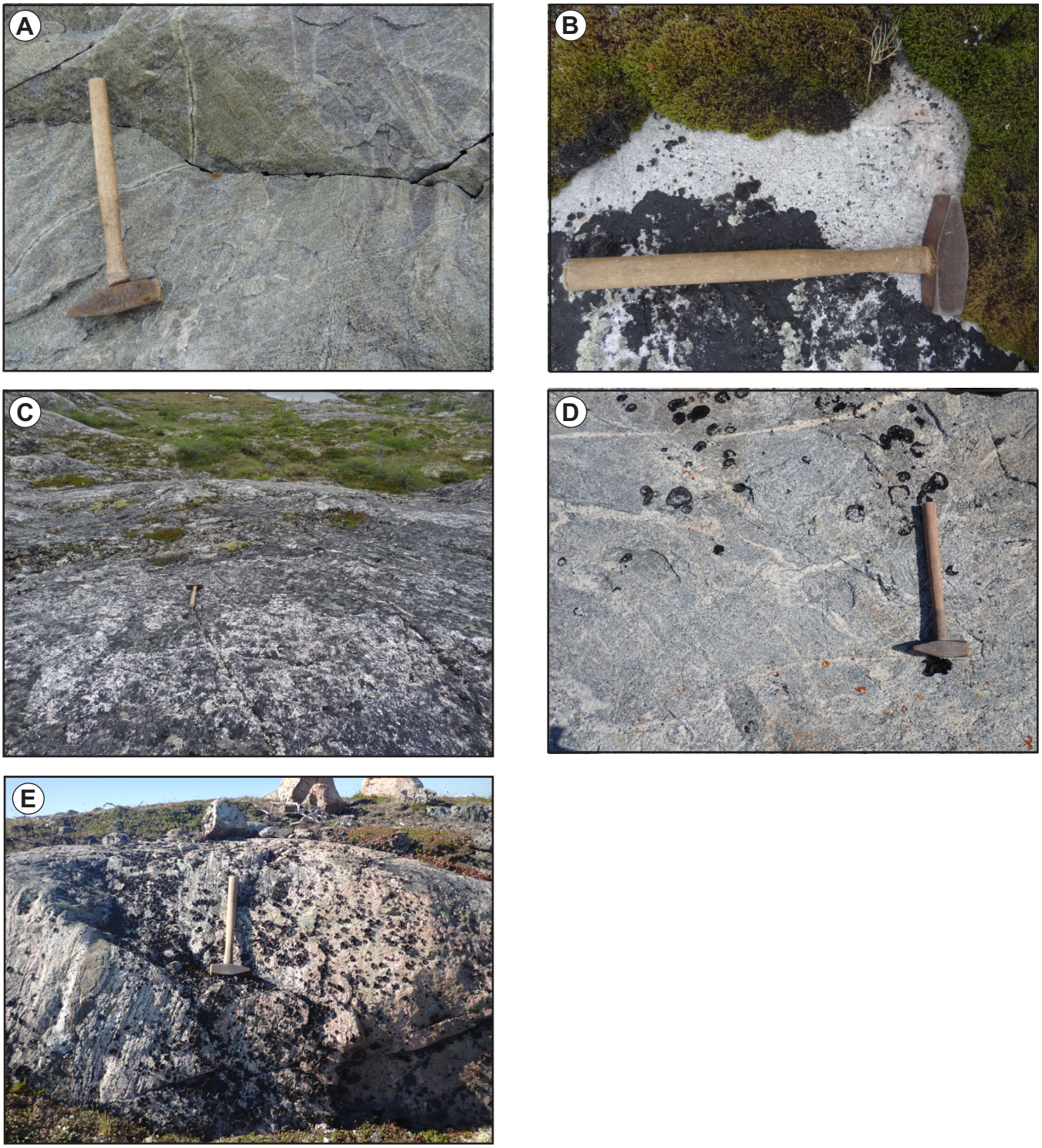

Plate 1. *Field photographs of the samples collected for U–Pb zircon dating. A) Psammite (19AH004A); B) Monzogranite (19AH002A); C) Granodiorite (19AH001A); D) Quartz diorite (21AH041A); E) Granodiorite (21AH105A). Hammer is 48 cm long.*

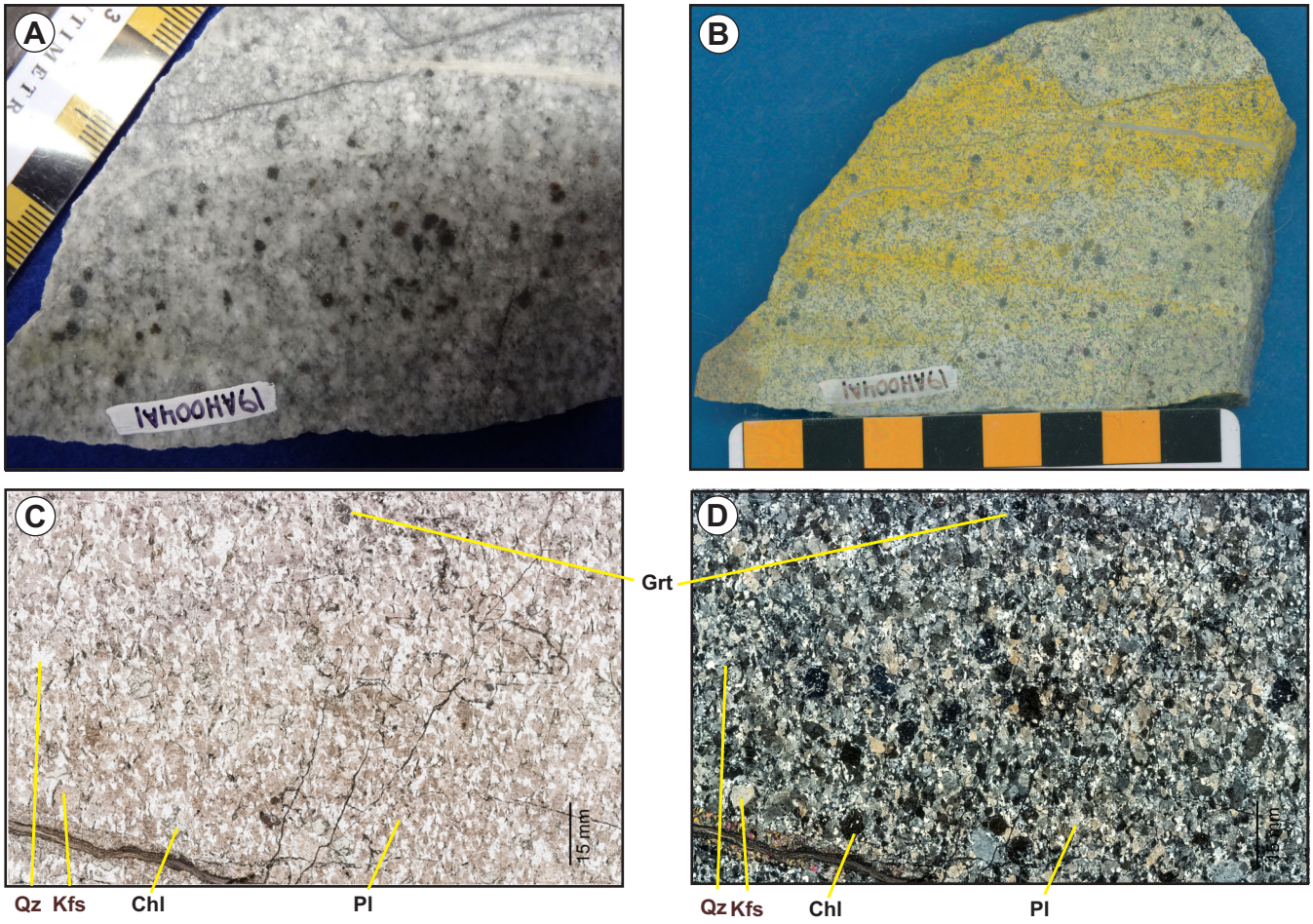

Plate 2. *A) Slab photograph; B) Stained slab photograph (K-feldspar is stained yellow); C, D) Photomicrographs (plane-polarized light and cross-polarized light) of the psammite geochronology sample (19AH004A). Grt=garnet, Pl=plagioclase, Chl=chlorite, Qz=quartz, Kfs=potassium feldspar.*

serpentinized ultramafic schists. The psammite and ultramafic rocks are infolded with a 3105+6/-9 Ma orthogneiss (Stevens *et al.*, 1982). The unit is along strike of the FLG and may represent part of that group.

In thin section, the psammite's primary minerals are plagioclase, quartz and potassium feldspar (Plates 2C, D and 3A). Accessory phases include chlorite, epidote, hornblende, muscovite, titanite, biotite, apatite, allanite and garnet. Retrograde chlorite occurs as subrounded poikiloblasts that are 1–2 mm in width and are commonly intergrown with epidote. Garnet grains are fractured and appear to be replaced by potassium feldspar, biotite, epidote and chlorite.

For a detrital population, zircon grains are mostly homogeneous in appearance, with most being clear and colourless prisms with an aspect ratio of 2:1 to 4:1 (Figure 3A, inset). Although some grains have slightly rounded facets/terminations, there is no evidence (frosted surface, highly rounded) of long-distance transport. In BSE/CL imagery, the grains are characterized by well-developed oscillatory zoning. Many grains consist of oscillatory zoned cores surrounded by a high U (CL dark/BSE bright), unzoned rims.

Sixty-nine SHRIMP analyses were carried out on 61 individual detrital zircon grains, yielding $^{207}Pb/^{206}Pb$ ages from 3153 to 2711 Ma. The oscillatory zoned zircon, both as discrete grains and cores yield $^{207}Pb/^{206}Pb$ ages between 3151–2978 Ma (Figure 3A). Most of these (~80%) form an unimodal population at 3140 Ma. A second minor mode appears on a cumulative probability distribution plot centred at *ca.* 3100 Ma. Because of the significant overlap between these two age components, an unmix function was used to statistically determine that the $^{207}Pb/^{206}Pb$ age of the youngest component is 3101 ± 5 Ma (function from Ludwig 2012). This represents the maximum age of deposition. The unmixing calculation incorporated all analyses of oscillatory

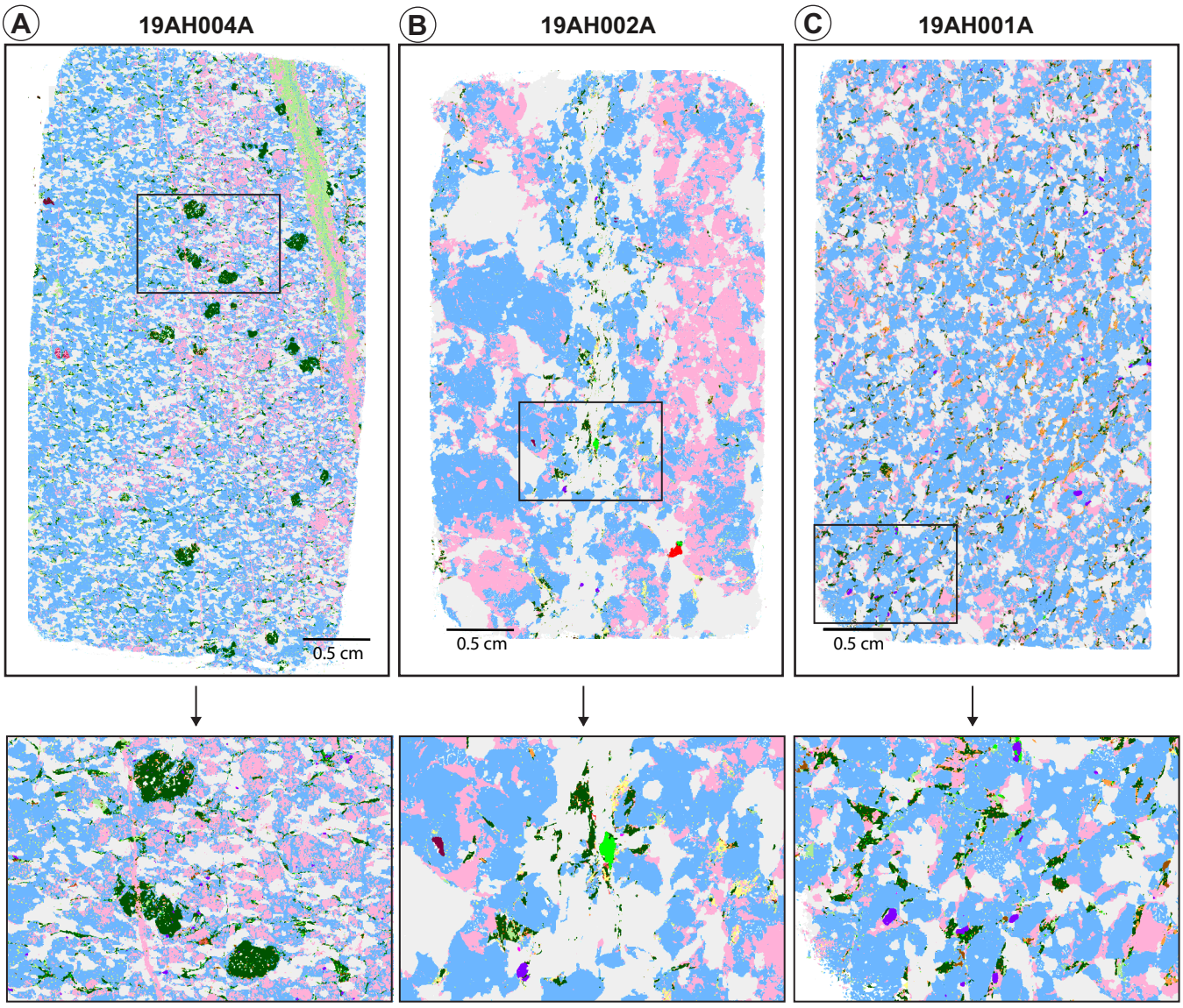

Weight Percentage(%) Samples	19AH004A	19AH002A	19AH001A
Quartz	30.02	36.54	28.65
Plagioclase	41.75	38.14	50.15
Chlorite	4.23	1.15	2.54
Biotite	0.22	0.11	1.75
Muscovite	0.53	0.79	0.51
K Feldspar	17.57	22.64	13.65
Calcite	0.01	-	-
Epidote	3.67	0.23	1.54
Hornblende–Fe	0.78	-	-
Rutile	0.01	-	-
Titanite	0.48	0.09	0.45
Apatite	0.23	0.04	0.24
Garnet	0.06	0.02	-
Clinopyroxene (Fe–Mg)	0.01	0.01	0.01
Allanite	0.33	0.06	0.47
Zircon	0.03	0.01	0.03
Chalcopyrite	-	-	-
Iron Oxide	-	0.12	0.01
Pyrite	-	-	-
Ilmenite	0.05	0.02	0.01

Plate 3. *False-colour SEM-MLA maps.Weight percent mineral proportions (recalculated from area percent) are indicated in table. A) Psammite (19AH004A); B) Monzogranite (19AH002A); C) Granodiorite (19AH001A); D) Quartz diorite (21AH041A); E) Granodiorite (21AH105A).*

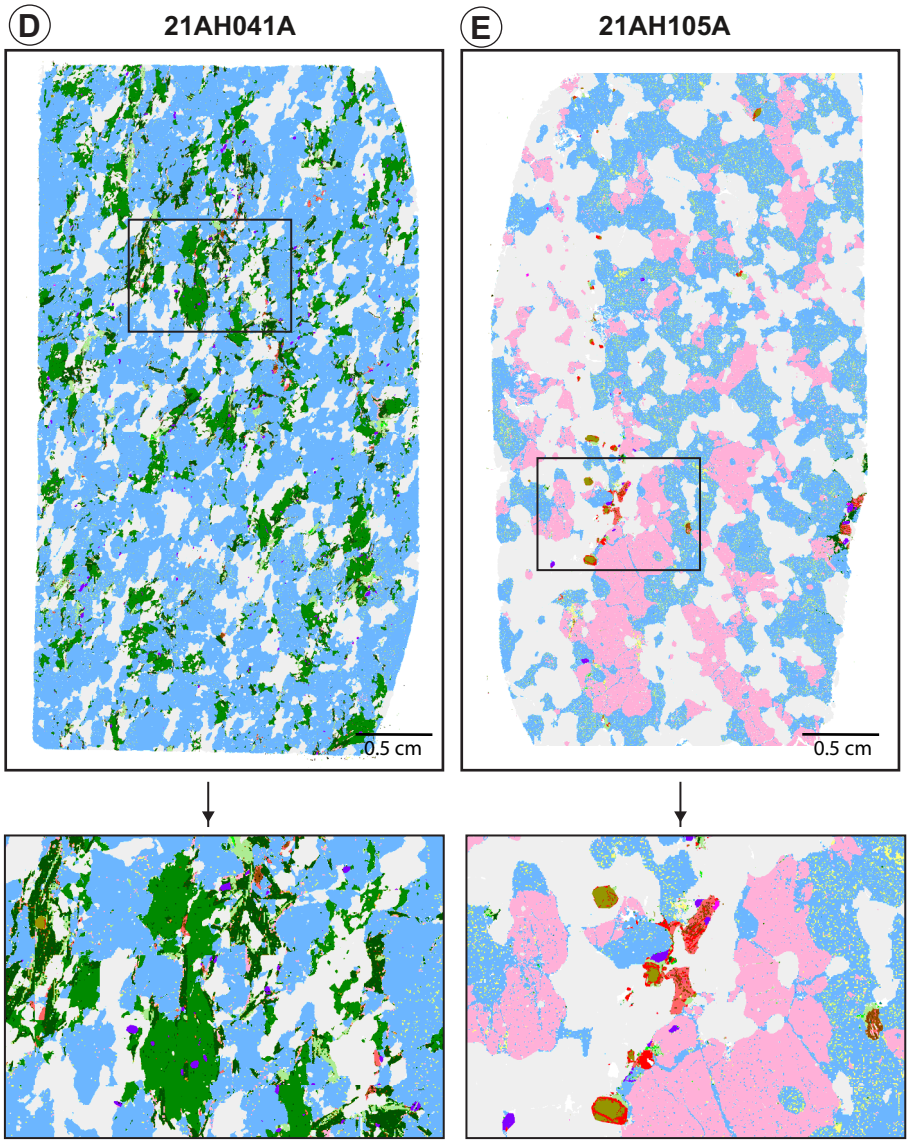

Weight Percentage(%) Samples	21AH041A	21AH105A
Quartz	22.70	42.42
Plagioclase	54.71	34.42
Chlorite	4.32	0.19
Biotite	0.17	-
Muscovite\Sericite	0.82	4.52
K Feldspar	0.89	16.79
Calcite	-	-
Epidote	2.34	0.45
Hornblende-Fe	12.91	0.05
Rutile	0.02	0.03
Titanite	0.32	0.07
Apatite	0.38	0.12
Garnet	-	-
Clinopyroxene (Fe-Mg)	0.01	0.01
Allanite	0.04	0.08
Zircon	0.02	0.02
Chalcopyrite	-	-
Iron Oxide	0.01	0.31
Pyrite	0.04	0.27
Ilmenite	0.27	0.18

Plate 3. *Continued.*

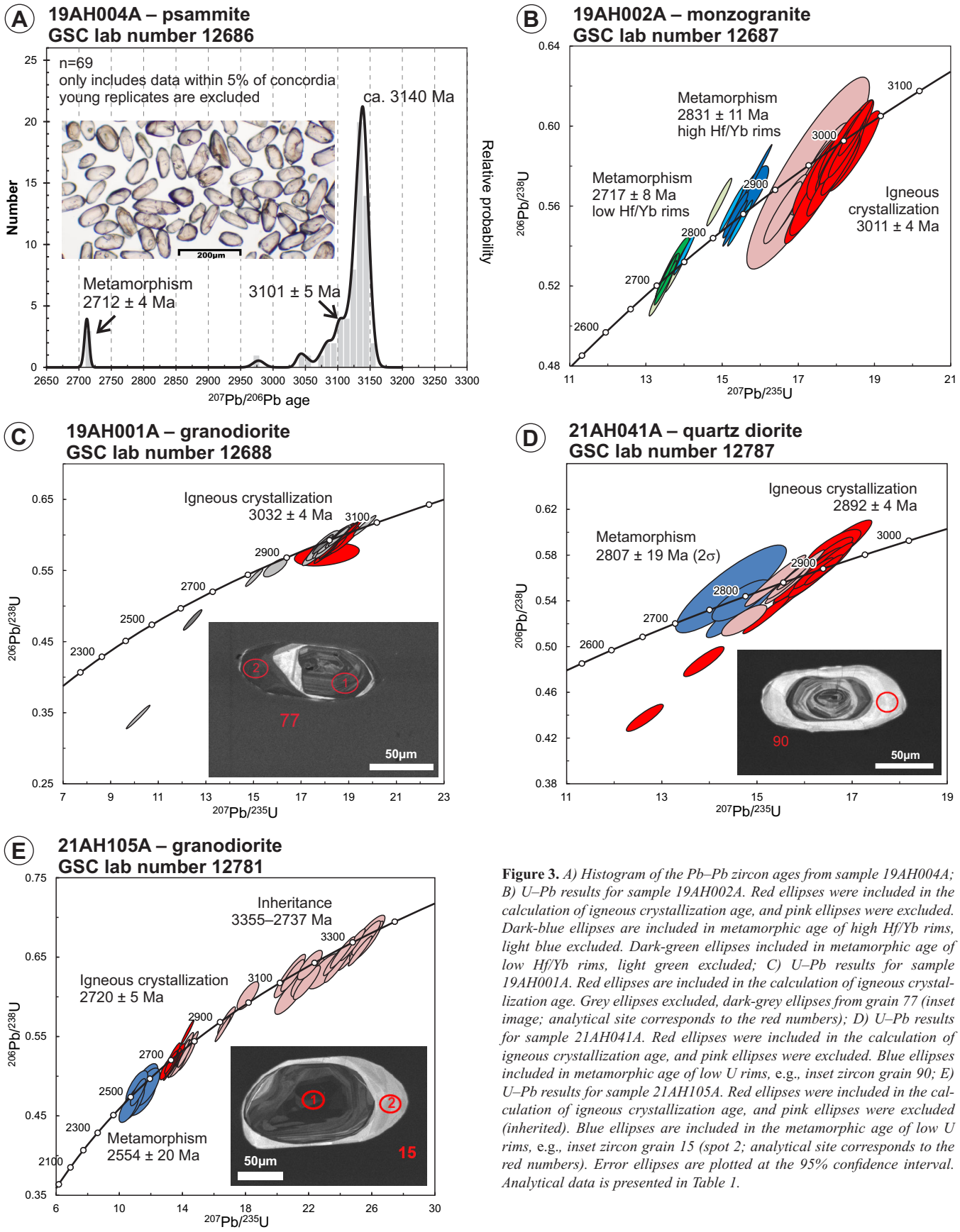

Figure 3. *A) Histogram of the Pb–Pb zircon ages from sample 19AH004A; B) U–Pb results for sample 19AH002A. Red ellipses were included in the calculation of igneous crystallization age, and pink ellipses were excluded. Dark-blue ellipses are included in metamorphic age of high Hf/Yb rims, light blue excluded. Dark-green ellipses included in metamorphic age of low Hf/Yb rims, light green excluded; C) U–Pb results for sample 19AH001A. Red ellipses are included in the calculation of igneous crystallization age. Grey ellipses excluded, dark-grey ellipses from grain 77 (inset image; analytical site corresponds to the red numbers); D) U–Pb results for sample 21AH041A. Red ellipses were included in the calculation of igneous crystallization age, and pink ellipses were excluded. Blue ellipses included in metamorphic age of low U rims,* e.g., *inset zircon grain 90; E) U–Pb results for sample 21AH105A. Red ellipses were included in the calculation of igneous crystallization age, and pink ellipses were excluded (inherited). Blue ellipses are included in the metamorphic age of low U rims,* e.g., *inset zircon grain 15 (spot 2; analytical site corresponds to the red numbers). Error ellipses are plotted at the 95% confidence interval. Analytical data is presented in Table 1.*

zoned zircon except young replicate analyses on three grains; only the oldest replicate analyses for a given grain were included. The three youngest analyses are from the high U rims and yield a weighted mean $^{207}Pb/^{206}Pb$ age of 2712 ± 4 Ma (MSWD = 0.105, probability of fit = 0.90). While these rims were commonly observed on most grains, most were too narrow to permit analysis, hence the low number of analyses (n) for the weighted mean age. However, their ubiquity is an indication that this age represents a metamorphic overprint on the psammite and not a detrital component.

Foliated Monzogranite (Sample 19AH002A; GSC Lab Number 12687)

The sample is from a medium- to coarse-grained, moderately to strongly foliated, recrystallized, biotite–hornblende monzogranite (Plate 1B). The outcrop is leucocratic, grey-weathering, envelopes m-wide ultramafic pods and is cut by amphibolite dykes (Kikkertavak dykes), and late cm-scale pegmatite veins and gabbro dykes (Harp dykes). The monzogranite locally preserves relict potassium feldspar augen (Plate 4A, B) and displays hornblende-facies metamorphism. The unit is folded, and locally sheared with an L-fabric that is commonly reoriented or folded into the plane of shear foliation.

In thin section, the major minerals are plagioclase, quartz, and potassium feldspar (Plates 3B and 4C, D). Accessory phases include chlorite, muscovite, magnetite and biotite. Grains display a granoblastic texture. Exsolution lamellae of potassium feldspar in plagioclase are preserved. Accessory minerals define a discontinuous foliation.

In plain-polarized light, zircons are characterized by an elongate prismatic morphology often comprised of a clear, colourless core surrounded by a pale-brown, slightly turbid rim. In CL images, oscillatory zoning is present in the cores of most grains, however, the rims have very poor CL response due to their high U content and partial alteration, which is more apparent in the corresponding BSE images.

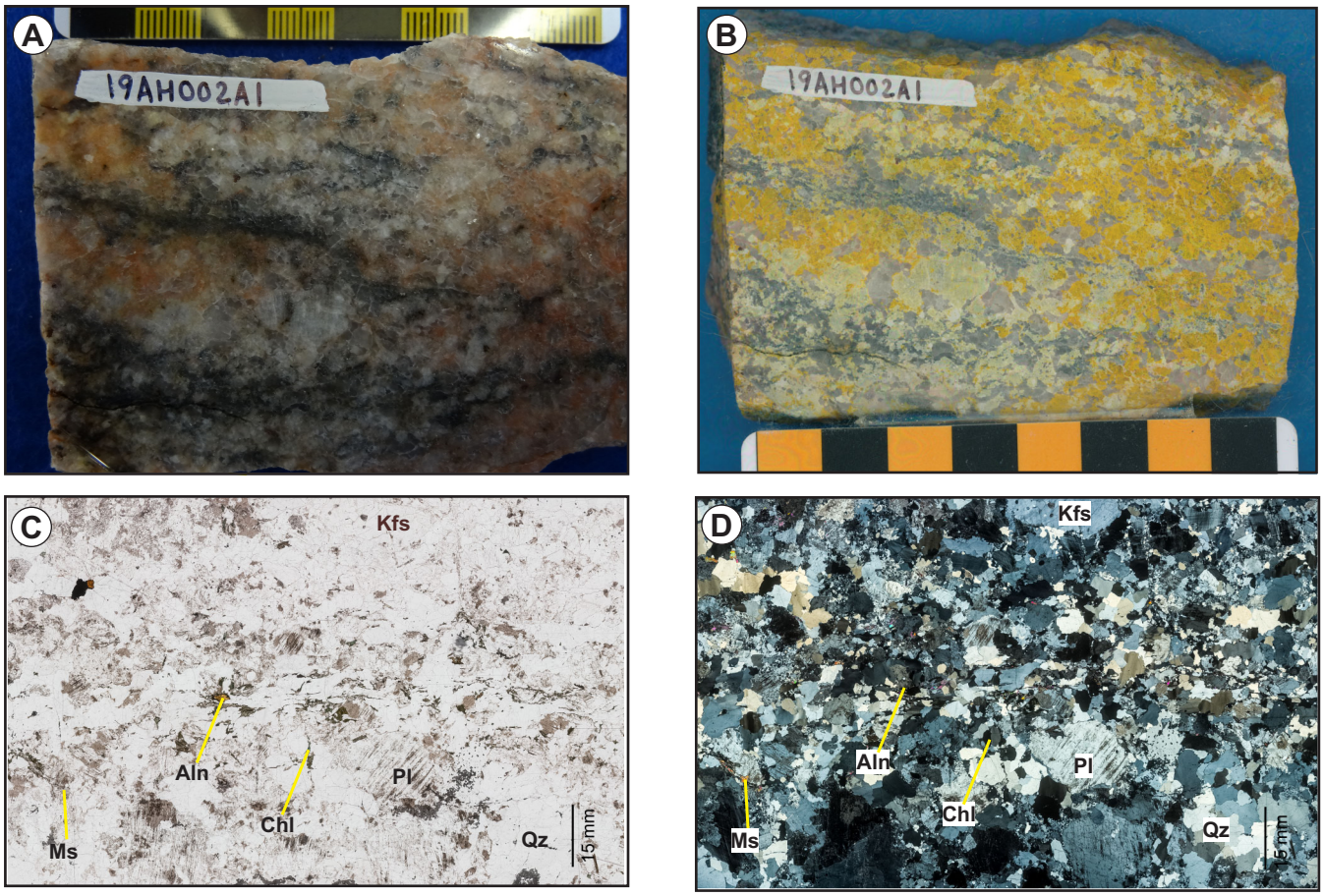

Plate 4. *A) Slab photograph; B) Stained slab photograph (K-feldspar is stained yellow); C, D) Photomicrographs (plane-polarized light and cross-polarized light) of the geochronology sample of monzogranite (19AH002A). Ms=muscovite, Aln=allanite, Pl=plagioclase, Chl=chlorite, Qz=quartz, Kfs=potassium feldspar.*

Thirty-seven SHRIMP analyses were conducted on 33 individual zircon grains. The oscillatory zoned zircon cores record the oldest ages from 3035 to 2952 Ma. The weighted mean $^{207}Pb/^{206}Pb$ age of the 18 oldest analyses is 3011 ± 4 (MSWD = 1.6, probability = 0.061), interpreted as the crystallization age of the monzogranite (Figure 3B). This excludes five slightly younger analyses interpreted to reflect Pb-loss during the polymetamorphic history of this sample. This complex metamorphic history is reflected in zircon overgrowths with two distinct ages at *ca.* 2.8 Ga and 2.7 Ga. There are no morphological differences between rims of different ages, nor is there any consistent variability in their U abundance or Th/U values. The only chemical difference is in their Hf/Yb values. Grains with higher Hf/Yb ratios (generally over ~105) form the older cluster, whereas those with lower Hf/Yb ratios form the younger cluster. There is some scatter within each cluster, four analyses of the high Hf/Yb ratios cluster and yield a weighted mean $^{207}Pb/^{206}Pb$ age of 2831 ± 11 Ma (MSWD = 5.9, probability of fit = 0.001). The youngest four analyses of the low Hf/Yb ratio group yield a weighted mean $^{207}Pb/^{206}Pb$ age of 2717 ± 8 Ma (MSWD = 1.9, probability of fit = 0.12).

Foliated Granodiorite (Sample 19AH001A; GSC Lab Number 12688)

The sample is from a medium-grained, moderately to strongly foliated, lineated, recrystallized, compositionally layered, biotite–hornblende granodiorite (Plates 1C, 5A, B). The rock is leucocratic, grey-weathering, heterogenous and has discontinuous compositional layering. The sample preserves amphibolite-facies metamorphism. Minor leucosome (<10%) is present, as are abundant 1- to 5-m wide, layered amphibolite (hornblendite) and anthophyllite–biotite altered ultramafic boudins and rafts. These boudins have previously been interpreted as part of the Weekes Amphibolite (Ermanovics, 1993). The unit occurs in the limbs of a megascopic (400 m wavelength) fold that plunges to the north.

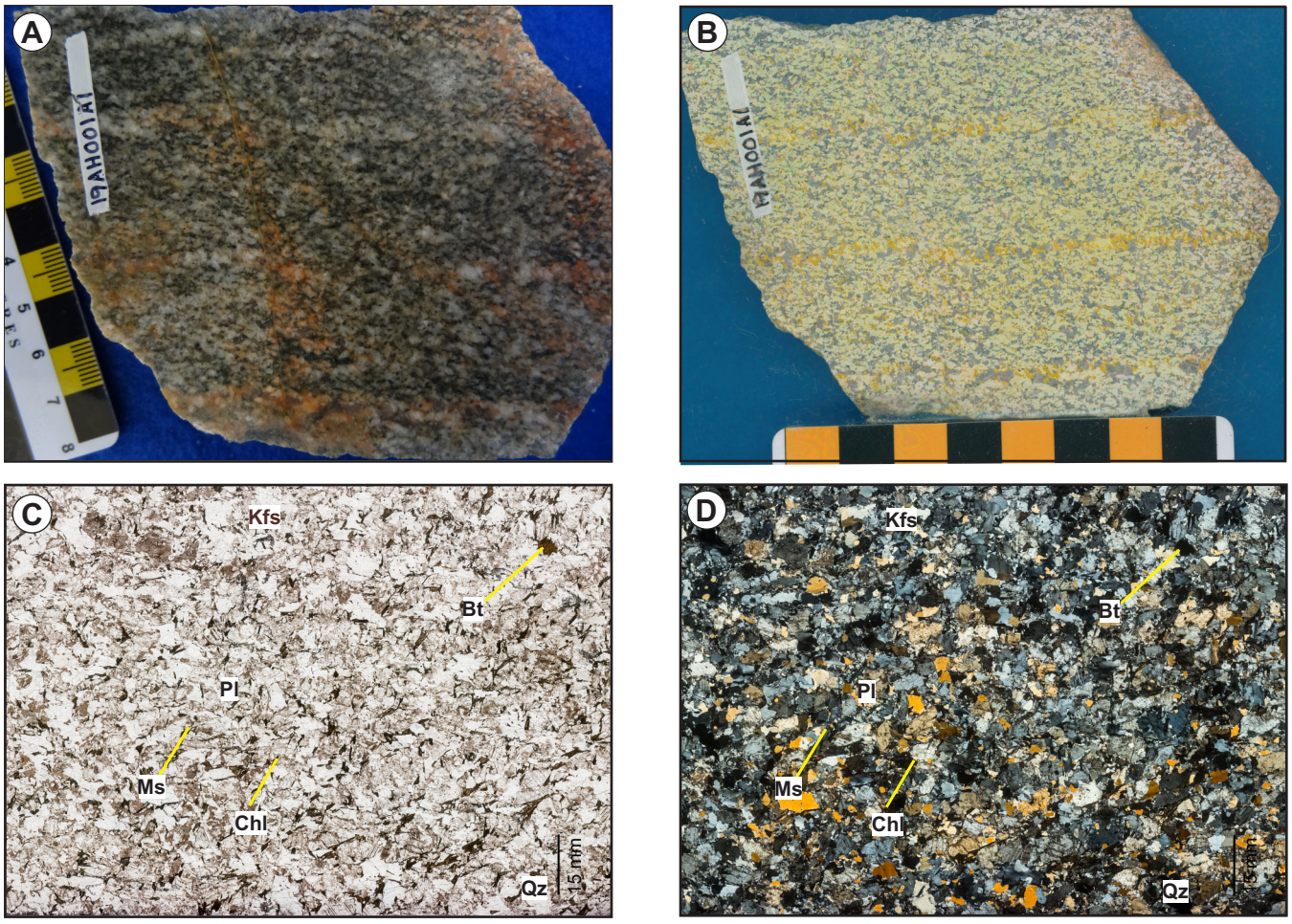

Plate 5. *A) Slab photograph; B) Stained slab photograph (K-feldspar is stained yellow); C, D) Photomicrographs (plane-polarized light and cross-polarized light) of the geochronology sample of granodiorite (19AH001A). Ms=muscovite, Bt=biotite, Pl=plagioclase, Chl=chlorite, Qz =quartz; Kfs, Potassium feldspar.*

In thin section, the main minerals are plagioclase, quartz and potassium feldspar and are typically 4–8 mm in length (Plates 3C and 5C, D). Accessory phases are chlorite, biotite, epidote and muscovite and are 0.5 to 2 mm in length. Trace amounts of titanite, allanite, and apatite also occur. Biotite is commonly rimmed by chlorite. Mafic minerals define the weakly developed foliation.

The recovered zircons are consistently pale brown, elongate prisms with concentric zoning and minor fracturing visible in plane light. Most grains exhibit well-developed oscillatory zoning in CL. Many grains contain fractures and may exhibit a BSE response typical of alteration in areas of high U abundance.

Thirty-one SHRIMP analyses were carried out on 25 individual zircon grains. The weighted mean $^{207}Pb/^{206}Pb$ age of 15 of the oldest analyses is 3032 ± 4 Ma (MSWD = 2.0, probability of fit) = 0.014 (Figure 3C). This excludes one slightly older analysis (3068 Ma) where the analytical spot may be nicking an older core. The age of crystallization of the granodiorite is interpreted as 3032 ± 4 Ma. Another 13 analyses are spread along concordia down to ~2840 Ma, and are interpreted to represent grains that have been affected by Pb-loss during alteration and/or metamorphism. One rim of a zircon grain yielded the youngest result at ~2720 Ma; however, it falls well off concordia (Figure 3C). Assuming a simple single stage of metamorphism such a discordant result would suggest metamorphism after ~2.7 Ga; however, given the complex metamorphic history of the area, no such firm conclusion is possible from this single analysis.

Quartz Diorite (Sample 21AH041A; GSC Lab Number 12787)

The sample is from the KIS and is a medium-grained, weakly to moderately foliated, moderately lineated, recrystallized hornblende quartz diorite (Plates 1D and 6A, B).

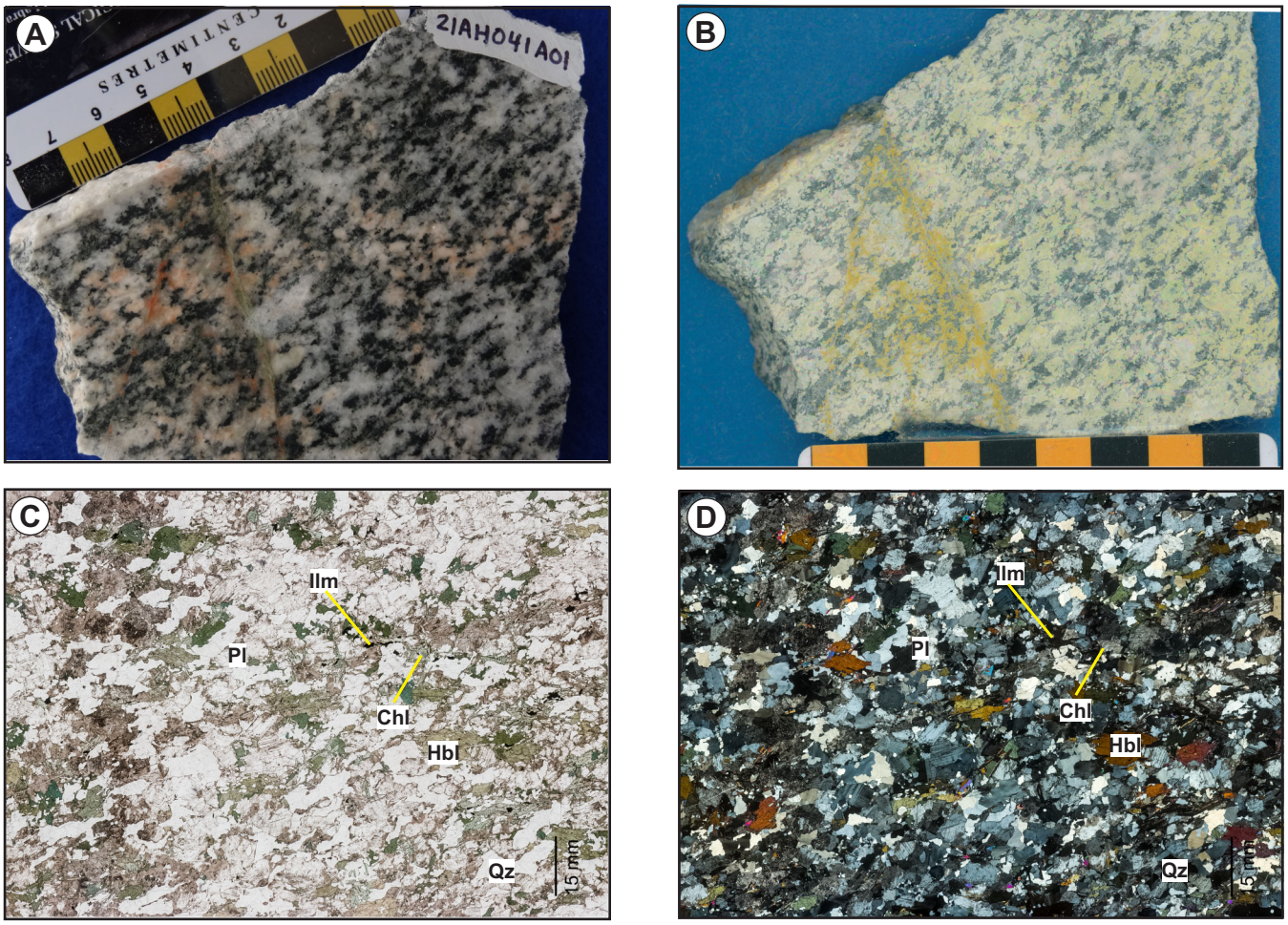

Plate 6. *A) Slab photograph, B) Stained slab photograph (K-feldspar is stained yellow); C, D) Photomicrographs (plane-polarized light and cross-polarized light) of the geochronology sample of quartz diorite (21AH041A). Pl=plagioclase, Chl=chlorite, Qz=quartz, Hbl=hornblende, Ilm=ilmenite.*

The outcrop is leucocratic, grey-weathering, with minor felsic, leucocratic, discontinuous veins (possible anatectic leucosome). The sample preserved hornblende-facies metamorphism. The outcrop locally contains xenoliths of older orthogneiss (likely Maggo Gneiss) and is cut by cm-scale pegmatite and epidote–quartz veins. The KIS is preserved as lenticular and elongated bodies with a weakly developed foliation along its margins suggesting emplacement during active tectonism.

In thin section, the major phases are plagioclase, quartz and hornblende (Plates 3D and 6C, D). Accessory phases include chlorite, epidote, biotite, potassium feldspar and muscovite. Hornblende is rimmed by chlorite and epidote is partly altered to chlorite. Trace ilmenite, apatite, titanite and rutile also also present. Mafic minerals define the weakly developed foliation.

The zircon grains are colourless to pale brown, slightly ovoid prisms. Pale-brown zircons are more commonly fractured. In plane-polarized light, thin overgrowths are locally observed. Well-developed oscillatory zoning is present in these zircon grains, and many consist of a high U (dark CL response) core surrounded by a thin low U (bright CL response) rim. Most rims are less than 10 μm wide.

Thirty SHRIMP analyses were carried out on 29 individual zircon grains yielding concordant $^{207}Pb/^{206}Pb$ ages between 2903 and 2746 Ma. The weighted mean of the 21 oldest analyses is 2892 ± 4 Ma (MSWD = 1.9, probability of fit = 0.007) and is interpreted as the crystallization age of the quartz diorite (Figure 3D). Three low U rims were sufficiently thick to permit SHRIMP analysis. These exhibit scatter beyond their analytical error but suggest a metamorphic overprint at 2807 ± 19 Ma (2σ, MSWD = 3.5, probability of fit = 0.030; Figure 3D inset). Six analyses of oscillatory zoned zircon with younger ages between 2870 and 2865 Ma were not included in the calculation of the crystallization age. These are interpreted to have been affected by Pb-loss related to metamorphism.

Granodiorite (Sample 21AH105A; GSC Lab Number 12781)

The sample is medium- to coarse-grained, pink-buff weathering, massive to weakly foliated or lineated granodiorite (Plates 1E and 7A, B) that locally preserves augen of potassium feldspar. Mafic minerals define the foliation. The granodiorite contains xenoliths of amphibolite that are 5–10 cm wide and foliation parallel. The unit is cut by younger granitic veins.

In thin section, the major phases are quartz, plagioclase and potassium feldspar (Plates 3E and 7C, D). The plagioclase grains are partially altered by sericite. Accessory phases include apatite, pyrite magnetite and ilmenite. The pyrite is typically rimmed by magnetite.

The zircon grains are highly variable, from clear and colourless with no inclusions or fractures to medium brown and highly fractured. In CL, most grains have well-developed oscillatory zoning. Some grains appear to have high U (CL dark) cores surrounded by CL dark, oscillatory-zoned rims, whereas others are surrounded by CL bright (low U), sector-zoned rims.

Forty-nine SHRIMP analyses were carried out on 41 individual zircon grains yielding concordant $^{207}Pb/^{206}Pb$ ages between 3355 and 2519 Ma. The youngest analyses are from the low U, sector zoned rims which return a weighted mean $^{207}Pb/^{206}Pb$ age of 2554 ± 20 Ma (n=7, MSWD = 0.94, probability of fit = 0.47). Given the sector zonation, this is interpreted as the age of metamorphism. The next cluster of zircon dates return a weighted mean $^{207}Pb/^{206}Pb$ age of 2720 ± 5 Ma (n=12, MSWD = 1.4, probability of fit = 0.18) and is interpreted as the igneous age of this monzogranite (Figure 3E). These analyses are from CL-dark, oscillatory-zoned zircon, either as cores to 2.55 Ga rims (*e.g.*, grain 15, Figure 3E, inset) or as CL-dark rims around even older cores (*e.g.*, grain 20). All older zircon analyses (2737–3355 Ma) are interpreted as inherited. These occur as entire grains, rims, or cores indicating a complex crustal source for the inherited zircon.

DISCUSSION

TIMING CONSTRAINTS

The geochronological constraints presented above can be coupled with recent U–Pb geochronological data (Rayner, 2022) and historical ages (Loveridge *et al.*, 1987; Schiøtte *et al.*, 1989; James *et al.*, 2002) to revise the geological framework of the Archean components of the Hopedale Block. A summary of all of the Archean U–Pb zircon geochronological data is presented in Table 1 and Figure 4. The main geological units and geochronological constraints are summarized below.

Paleoarchean

3262–3245 Ma

Maggo Gneiss

The 3262–3245 Ma magmatic event comprises the three mappable components of the Maggo Gneiss. They are migmatitic orthogneiss, granodioritic orthogneiss, and tonalitic orthogneiss. U–Pb zircon data from two samples of

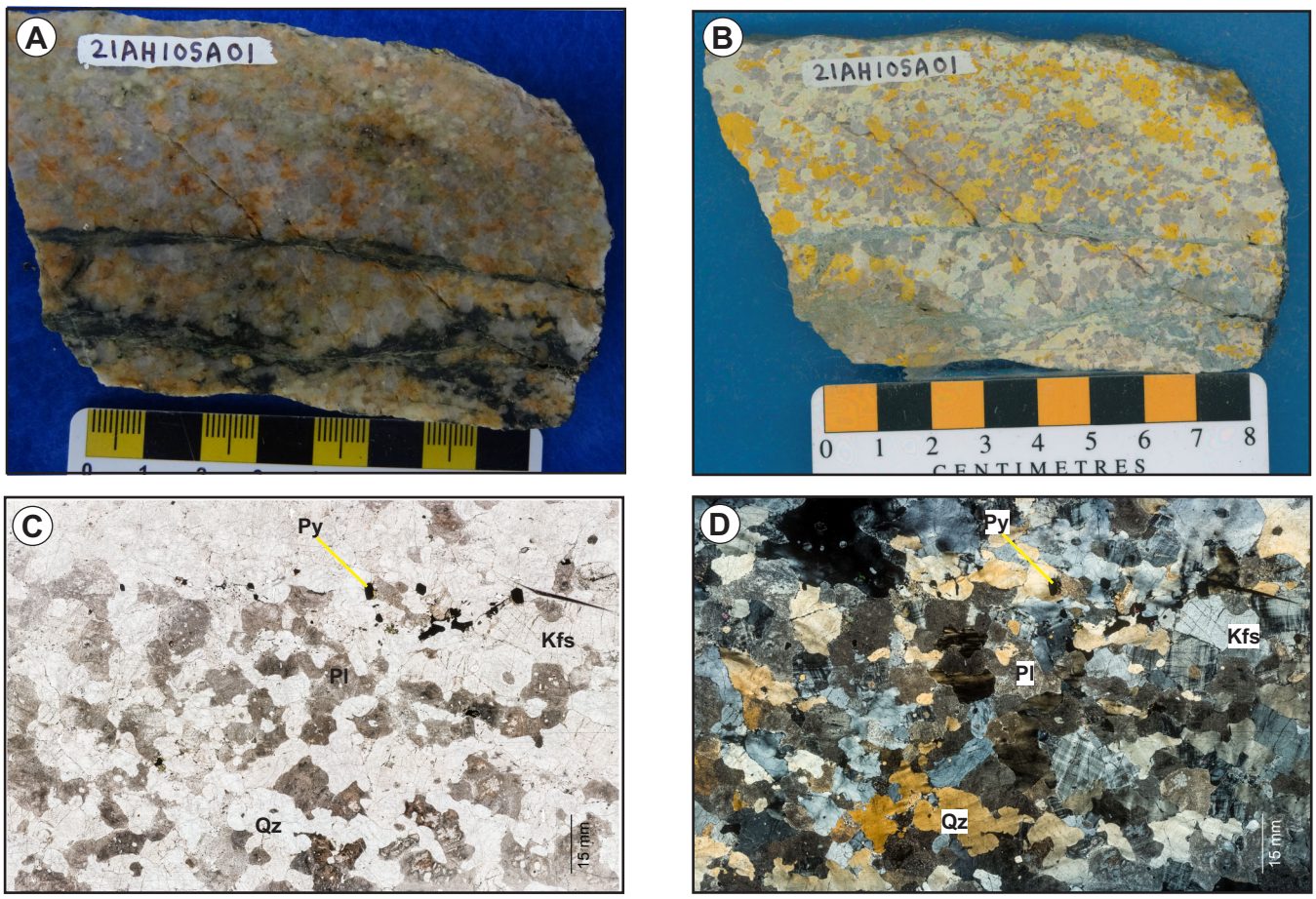

Plate 7. *A) Slab photograph; B) Stained slab photograph (K-feldspar is stained yellow); C, D) Photomicrographs (plane-polarized light and cross-polarized light) of the geochronology sample of granodiorite (21AH105A). Pl=plagioclase, Qz=quartz, Kfs=potassium feldspar, Py=pyrite.*

migmatitic orthogneiss yielded ages of 3247 ± 12 and 3258 ± 10 Ma with metamorphic overgrowths at 2833 ± 9 Ma (zircon) and *ca.* 2700 Ma (titanite) for the first sample, and 2846 ± 7 Ma for the second sample (Rayner, 2022). A sample from the tonalitic orthogneiss yielded a U–Pb zircon age of 3262 ± 5 Ma and metamorphic overgrowths at 2836 ± 4 Ma (zircon) and 2704 ± 4 Ma (titanite; Rayner, 2022). The boudinaged amphibolite within the Maggo Gneiss may represent the 'Hopedale dykes' of Ermanovics (1993), although the authors found that the presence of boudinaged amphibolite is not exclusively diagnostic of the Maggo Gneiss.

Supracrustal Rocks

A belt of diopside–garnet amphibolite and minor ultramafic and metasedimentary rocks is also included as a part of the 3262–3245 Ma event, as they are engulfed by the Maggo Gneiss. Although limited geochronological data exists for this unit, it occurs as rafts and xenoliths in the Maggo Gneiss and has historically been incorporated with the Weekes Amphibolite (Ermanovics, 1993). Geochronological studies and mapping as part of this research project recognized that multiple geological events are incorporated into what has been previously referred to as the Weekes Amphibolite (also *see* Sandeman *et al.*, 2023), and thus the term needs to be redefined or abandoned. An ion-probe U–Th–Pb zircon date from a metapelite contained detrital low-U zircon with a youngest age of 3258 ± 24 Ma (Schiøtte *et al.*, 1989). These data indicate the deposition of sedimentary rocks after *ca.* 3258 Ma. The lack of younger detrital zircon, coupled with the unit being engulfed in the Maggo Gneiss, suggests that this package of rocks may be older than 3245 ± 5, the youngest age of the Maggo Gneiss (Table 1). Further evidence for a volcanosedimentary belt older than *ca.* 3262 Ma comes from the above-dated Maggo Gneiss sample (3262 ± 5 Ma; Rayner, 2022). In the field, this gneiss was interpreted to crosscut a raft of volcanosedimentary rocks thought to be part of the FLG. This initial observation has not been revisited, but if this is correct, then the outlier is not part of the FLG and is >3262 Ma.

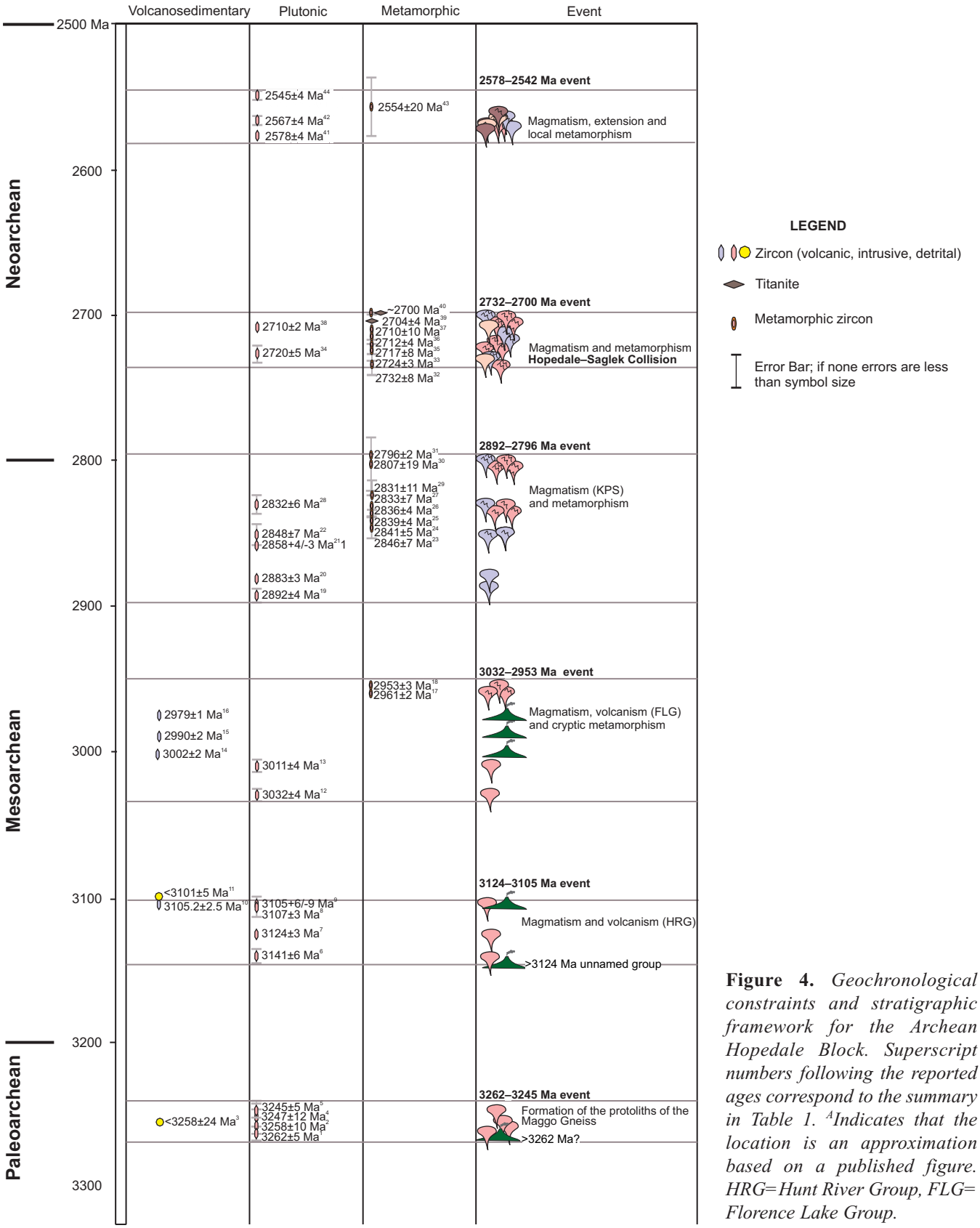

Figure 4. *Geochronological constraints and stratigraphic framework for the Archean Hopedale Block. Superscript numbers following the reported ages correspond to the summary in Table 1. [A]Indicates that the location is an approximation based on a published figure. HRG=Hunt River Group, FLG=Florence Lake Group.*

Mesoarchean

3141 to 3105 Ma

Unnamed Unit

The timing of the formation and genetic association of this previously unrecognized belt of volcanosedimentary rocks and contemporaneous intrusions remains uncertain. Based on field relationships, the volcanosedimentary rocks are younger than the *ca.* 3262–3245 Ma Maggo Gneiss. This belt includes a metamorphosed ultramafic unit, a metabasalt (locally amphibolite) and a package of metasedimentary rocks. These units were previously assigned to the HRG (Ermanovics, 1993); however, recent geochronology indicates that the metabasalt is cut by tonalite that has a U–Pb zircon date of 3124 ± 3 Ma (Rayner, 2022) and thus is older than the HRG that yielded a U–Pb zircon date of 3105.2 ± 2.5 Ma from a rhyolite sample from the southern part of the HRG (James *et al.*, 2002). An alternative interpretation is that the HRG is a longer lived volcanic event than previously recognized and that the belts in the northeast are older than the belts in the southwest.

Several biotite–hornblende tonalite and granodiorite intrusions are also included in this magmatic event. South of the community of Hopedale, a U–Pb zircon TIMS age of 3105+6/-9 Ma was reported from a hornblende orthogneiss (Loveridge *et al.*, 1987). A U–Pb zircon TIMS age of 3107 ± 3 Ma is also reported from tonalitic orthogneiss adjacent to the HRG (James *et al.*, 2002). The areal distribution of these ages suggests that this magmatic event was widespread throughout the Hopedale Block.

Hunt River Group

The HRG comprises ultramafic rocks, biotite ± garnet metabasalt, a composite metasedimentary unit and minor metarhyolite. Despite the areal extent of the group only one geochronological age exists. A rhyolite sample from the southern HRG yielded a U–Pb zircon TIMS date of 3105.2 ± 2.5 Ma (James *et al.*, 2002). A zircon overgrowth on this sample yielded a U–Pb zircon TIMS date of 2961 ± 2 Ma and is interpreted as the age of metamorphism of the rhyolite (James *et al.*, 2002).

3032 to 2953 Ma

Unnamed Units

Several unnamed units are part of this suite and are composed of biotite–hornblende migmatitic orthogneiss that ranges in composition from tonalitic to dioritic. This foliated, metatexitic, migmatitic orthogneiss contains abundant 5- to 20-m-wide amphibolite lozenges. The newly reported U–Pb zircon SHRIMP ages of 3032 ± 3.9 Ma (granodiorite - 19AH002A) and 3011 ± 4 Ma (tonalite - 19AH001A) are the first evidence of a magmatic event of this age. This event may, in part, be contemporaneous with the FLG; although, the current geochronological data suggest that the latter is slightly younger.

Florence Lake Group

The FLG comprises volcanic rocks (mafic and lesser felsic), metasedimentary rocks (pelites, chert and minor marble) and meta-ultramafic rocks (James *et al.*, 2002; Diekrup *et al.*, 2023). Geochronological constraints for this group include two quartz-phyric rhyolites that yielded TIMS U–Pb zircon dates of 2979 ± 1 and 2990 ± 2 Ma (James *et al.*, 2002). A TIMS U–Pb zircon date of 3002 ± 2 was reported from an additional rhyolite sample (Wasteneys *et al.*, 1996), although the precise location of the analyzed sample is not known. The sample of psammite (19AH004A), presented above, yielded a maximum age of deposition of 3101 ± 5 Ma and is herein interpreted as being part of the FLG. This is, in part, because the analyzed sample occurs along strike of the belt and it is lithologically similar to psammitic rocks of the FLG.

2892 to 2796 Ma

Kanairiktok Intrusive Suite

The KIS comprises two units: a) metatonalite with minor quartz diorite and; b) metamonzogranite to metagranodiorite. Published U–Pb zircon TIMS ages include 2858 +4/-3 Ma from a tonalitic phase (Loveridge *et al.*, 1987) and 2832 ± 6 Ma from a granodiorite phase (Rayner 2022). The newly reported U–Pb SHRIMP age of 2892 ± 4 from a quartz diorite phase further illustrates the regional distribution of this suite. In addition, evidence of associated metamorphism is preserved in many geochronology samples as overgrowths on zircons (Table 1; Figure 4).

Neoarchean

2732 to 2700 Ma

Unnamed Units

Two new magmatic pulses are recognized as belonging to this event. A sample, near the community of Hopedale, of a medium-grained granite vein yielded a U–Pb zircon SHRIMP crystallization age of 2710 ± 2 Ma (Rayner, 2022). This vein crosscuts a biotite ± hornblende tonalitic orthogneiss with a U–Pb zircon SHRIMP age of 3124 ± 3 Ma. In the western Hopedale Block, a new U–Pb SHRIMP

age of 2720 ± 5 Ma from a weakly foliated, quartz diorite pluton illustrates the regional extent of magmatism. In addition, evidence of a *ca.* 2732–2700 Ma metamorphism is preserved in many samples as both overgrowths on zircons and titanite ages (Table 1; Figure 4).

2578 to 2545 Ma

Aucoin Plutonic Suite

The Aucoin Plutonic suite comprises at least three phases: syenogranite to monzogranite, monzodiorite, and alkali gabbro; only the syenogranite phase is weakly foliated and lineated. Herein, the white-weathering, muscovite + biotite + tourmaline pegmatites mapped by James (1997) are included with the Aucoin Plutonic suite. The pegmatites intrude the HRG, but are themselves foliated. Based on the field descriptions provided by James (1997), the pegmatites most closely resemble the Aucoin Plutonic suite. A U–Pb zircon TIMS crystallization age of 2567 ± 4 Ma was determined from a syenitic phase of the suite (Sandeman and McNicoll, 2015). The *ca.* 2720 Ma quartz diorite, presented above (sample 21AH105A), preserved evidence of a 2554 Ma metamorphism (zircon overgrowths). There are two additional plutons recognized as part of this suite that have U–Pb zircon ages of *ca.* 2580 and *ca.* 2573 Ma with zircon overgrowths at *ca.* 2542 Ma (N. Rayner, unpublished data, 2024). U–Pb TIMS dates of 2578 ± 2 and 2545 ± 4 Ma from granite samples were reported by Wasteneys *et al.* (1996) suggesting a widespread magmatic event, at least in the western part of the Hopedale Block. These dated granites are considered to be part of the Aucoin Plutonic suite.

NEW TECTONIC FRAMEWORK

The new geochronological data presented herein, coupled with previously published data collected as part of this project (Rayner, 2022), better constrain the evolution of the Hopedale Block (Figures 4 and 5). Early models interpreted the HRG as the oldest volcanosedimentary belt in the region and all the remaining rafts of amphibolite, metasedimentary and ultramafic units engulfed by gneissic and intrusive rocks (*i.e.*, Maggo Gneiss and KIS) were termed Weekes Amphibolite (Ermanovics, 1993; Wasteneys *et al.*, 1996). Based on lithogeochemistry and isotopic data, Sandeman *et al.* (2023) illustrated that some of the rafts are dismembered remnants of the HRG but some Nd isotopic evidence suggests an older component. Based on the geochronology, those observations are further validated, demonstrating that the Paleoarchean–Mesoarchean volcanosedimentary history of the area is more complex than previously realized. Herein, it is recognized that some of these rafts/belts of amphibolite, ultramafic and metasedimentary rocks form part of a 3262–3245 Ma volcanosedimentary and intrusive event and are thus older than the HRG. Clearly, under its present definition, rocks of differing ages and origins are presently incorporated into the Weekes Amphibolite: the term needs to be redefined or abandoned. The oldest ages thus far reported in the Hopedale Block are from the Maggo Gneiss, which herein is redefined as a 3262–3245 Ma magmatic event consisting dominantly of gneissose tonalite ranging locally to granodiorite. The maximum age of deposition for a metasedimentary rock engulfed by the Maggo Gneiss is *ca.* 3258 Ma. The lack of younger detrital zircon, coupled with the youngest age of the host gneiss being *ca.* 3245 ± 5 Ma, suggests that there is a supracrustal package of rocks older than 3245 Ma. Further evidence for an older belt of volcanosedimentary rocks is from field observations indicating that the oldest, dated *ca.* 3262 Ma, gneiss cuts an older volcanosedimentary raft (Rayner, 2022). If this interpretation is correct, then the dispersed rocks of this belt represent the oldest in the region; however, it is herein suggested that additional geochronology of the volcanosedimentary sequence crosscut by the *ca.* 3262 Ma gneiss is required to substantiate this assertion. This is because the dated *ca.* 3262 Ma gneiss has a complex zircon population that also contains a population of zircon defining a 2836 ± 4 Ma event. Rayner (2022) interpreted the older zircons as representing the crystalization age based on their uniform age distribution and zircon morphology; however, the possibility exists that *ca.* 2836 Ma is the crystalization age. Given the significance of the age with respect to the minimum age of the volcanosedimentary package further geochronology is warranted.

Post *ca.* 3245 Ma, there is a break in the rock record until the *ca.* 3141–3105 Ma intrusive, volcanic and sedimentary events. This interval saw at least three distinct pulses of plutonism at 3141 ± 6, 3124 ± 3 and 3107 ± 3 Ma. The youngest age of plutonism corresponds to the timing of volcanism in the HRG, which is therefore also included in this event. In addition, a newly recognized volcanosedimentary belt is also included in this event. This is a package of metamorphosed ultramafic rocks, metabasalt (locally amphibolite) and metasedimentary rocks that were previously considered part of the HRG (Ermanovics, 1993). New geochronology indicates that the metabasalt is cut by tonalite that has a U–Pb zircon date of 3124 ± 3 Ma (Rayner, 2022) and thus is older than the HRG, which has a U–Pb zircon date of 3105.2 ± 2.5 Ma from a rhyolite sample (James *et al.*, 2002). As such, it is herein proposed that this belt is older than >3124 Ma and thus not part of the HRG as currently defined. An alternative hypothesis is that the HRG represents a long-lived volcanic event where older units are preserved in the northeast and it youngs to the southwest. Additional isotopic and geochronological data would be required to differentiate between these two hypotheses.

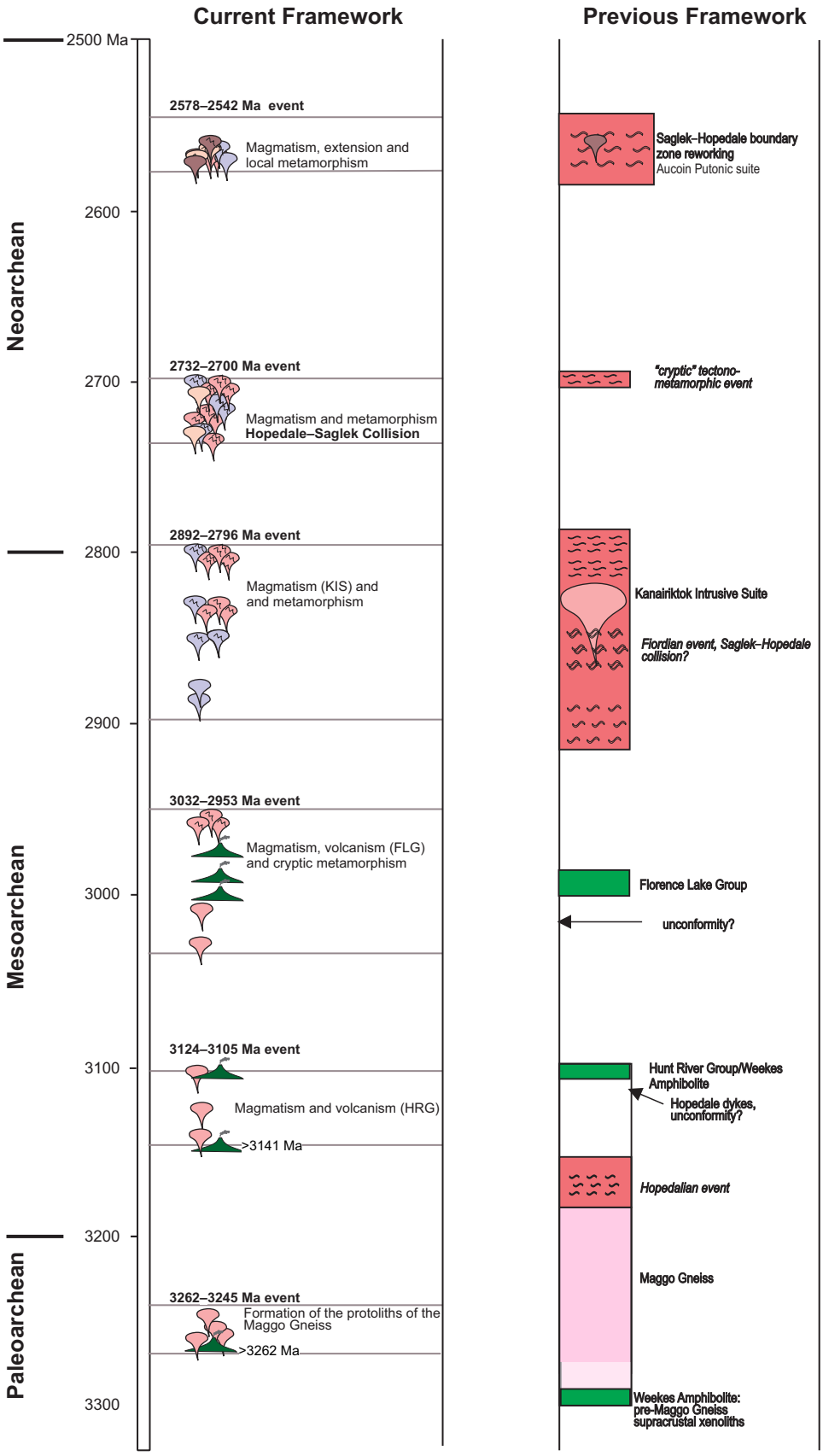

Figure 5. *Comparison between the current tectonic framework proposed herein, and the previous most recent framework proposed by Sandeman* et al. *(2023). HRG=Hunt River Group, FLG=Florence Lake Group, KIS=Kanairiktok Intrusive Suite.*

There is an approximately 70 m.y. hiatus in magmatism until the *ca.* 3032–2953 Ma thermal-magmatic event (Figure 4). This event includes a newly recognized and as yet unnamed plutonic suite that formed between *ca.* 3032 and 3011 Ma. Deposition of the FLG occurred during this event interval from *ca.* 3003–2979 Ma. The dated psammite (presented above), yielded a maximum age of deposition of 3101 ± 5 Ma and is therefore likely part of the FLG. This interpretation is based on the location of the psammite along strike of the FLG and its lithological similarity to the units in the group. The lack of zircon younger than *ca.* 3101 Ma could be explained as either: a) a very local source of sediment or; b) a lack of magmatic activity and erosion between 3101 Ma and deposition of the FLG at *ca.* 3000 Ma. Plutonism may, in part, be contemporaneous with the FLG; although current geochronological constraints suggest that the FLG is slightly younger. Evidence for a cryptic *ca.* 2961–2953 Ma metamorphic overprint associated with this event is documented as zircon overgrowths in a sample from the Maggo Gneiss and from a sample of the *ca.* 3107 Ma orthogneiss. The 2.95 Ga metamorphic event is only preserved in two samples and likely represents a localized event.

The next recorded thermal-magmatic event, from *ca.* 2892–2796 Ma, comprises the widespread and relatively long-lived formation of the KPS. Geochronological data indicate that magmatism occurred from 2892 ± 4 to at least 2832 ± 6 Ma, with some evidence of a metamorphism occurring synchronously with the later phases of magmatism at *ca.* 2846 Ma and outlasting plutonism till *ca.* 2796 Ma. This metamorphic event is documented as overgrowths on zircon grains in multiple samples (Figure 4; Table 1). Widespread metamorphism following significant crustal growth with the intrusion of the KIS may signify the transition to a modern (*i.e.*, subduction driven) plate tectonic regime. In this setting, the KIS would document the first continental arc in the Hopedale Block.

The penultimate event is a *ca.* 2732–2700 Ma thermal-magmatic event documented in both the eastern and western Hopedale Block. Magmatism associated with this includes a newly documented *ca.* 2720 Ma granodiorite intrusion in the west and a *ca.* 2710 Ma granite vein in tonalite gneiss in the east. Although magmatism of this age is sparse, evidence of a synchronous metamorphic event from *ca.* 2732–2700 Ma is preserved in multiple samples across the block as both zircon overgrowths and new titanite grains (Figure 4).

The final documented Archean event in the Hopedale Block is the intrusion of the Aucoin Plutonic suite and an associated cryptic metamorphic event. There is one pluton dated at 2567 ± 4 Ma and zircon overgrowths at 2554 ± 20 Ma from a *ca.* 2720 Ma pluton suggest a contemporaneous metamorphic event. This is supported by the two additional magmatic ages of *ca.* 2580 and *ca.* 2573 Ma with zircon overgrowths at *ca.* 2542 Ma (Rayner, unpublished data, 2024). The aerial extent of this igneous/metamorphic event is uncertain. Similar ages of 2578 ± 2 and 2545 ± 4 Ma from granite samples were reported by Wasteneys *et al.* (1996) and correlated with similar aged, low-volume granitoids and metamorphism in the Saglek Block (Connelly and Ryan, 1999); this was suggested as evidence for the timing of collision between the Saglek and Hopedale blocks. It is noted herein that the boundary between the Hopedale Block and Southeastern Churchill Province also occurs in this area, complicating the tectonic history. If the collision of the Saglek–Hopedale blocks occurred at *ca.* 2560 Ma as suggested by Connelly and Ryan (1996) and Wasteneys *et al.* (1996), then there is little record of the collision in the Hopedale Block.

HOPEDALE BLOCK EVOLUTION AND IMPLICATIONS ON THE ASSEMBLY OF NAC

In comparing previous interpretations of the Hopedale Block, the new geochronological data support significant revisions to the tectonic model (Figure 5). Although the Maggo Gneiss is still regarded as a significant temporal component of the Hopedale Block, the formation of its protoliths is now restricted to the interval *ca.* 3262–3245 Ma. The age of the oldest supracrustal rocks is still uncertain; however, there is geochronological evidence for rocks older than *ca.* 3262 Ma and older than *ca.* 3141 Ma. Although the precise ages of these rocks are still uncertain, they are older than those of the *ca.* 3105 Ma HRG. No obvious evidence of the >3100 Ma Hopedalian metamorphism has been uncovered and hence, it is herein suggested that there was no Hopedalian metamorphic event.

Further refinements to the tectonic framework of the Hopedale Block include the recognition of magmatism preceding and following the prolonged volcanism associated with the formation of the FLG; although the significance of the cryptic *ca.* 2961–2953 Ma metamorphism is uncertain. In addition, the extent of the KIS has been further defined as a long-lived (*ca.* 2892–2832 Ma) magmatic event. It is now postulated that the KIS likely represents a continental magmatic arc that intruded the Hopedale Block; potentially denoting the first evidence of modern-style (*i.e.*, subduction driven) plate tectonics in the region. Associated metamorphism is, in part, contemporaneous with, and subsequent to, the intrusion of the KIS. Whether this event reflects the Fiordian metamorphic event that Ermanovics (1993) attributed to forming the penetrative fabric in the southeastern Hopedale Block is uncertain. Evidence against the Fiordian event being *ca.* 2846–2796 Ma, or perhaps the existence of

a Fiordian event, is that this age of metamorphism occurs throughout the Hopedale Block and is not limited to the "Fiordian zone" outlined by Ermanovics (1993). Alternatively, this *ca.* 2846–2796 Ma metamorphism may mark the collision of an enigmatic Archean crustal block to the Hopedale Block; however, it is unlikely to reflect the collision of the Saglek Block as correlative metamorphic events are not recognized herein during this interval (Figure 6; Schiøtte *et al.*, 1989; Wasteneys *et al.*, 1996; Dunkley *et al.*, 2019).

A widespread *ca.* 2732–2700 Ma metamorphic event coupled with a magmatic event is also now recognized. The widespread occurrence of this metamorphic event in both the Hopedale and Saglek blocks indicates a shared event and it is suggested that this marks the collision of the Saglek and Hopedale blocks (Figure 6). This is supported by recent work in the Saglek Block that illustrates two distinct high-temperature tectonothermal events at *ca.* 2750–2700 Ma and *ca.* 2550–2510 Ma (Kusiak *et al.*, 2018; Dunkley *et al.*, 2019). Whereas the tectonothermal activity at *ca.* 2.7 Ga is widely documented in the Saglek Block, the known extent of the *ca.* 2.5 Ga high-T metamorphism and deformation is more limited. It has been suggested that the latter is restricted to reworking the margins of the NAC (Dunkley *et al.*, 2019). Similar to the Saglek Block, the extent of the *ca.* 2.5 Ga metamorphism in the Hopedale Block is limited.

CONCLUSIONS

New geochronological data for the Hopedale Block of the NAC help to further refine the Archean tectonic evolution of the region, punctuated by several plutonic, volcanosedimentary and metamorphic events. The oldest dated rocks in the Hopedale Block are those of the variably deformed, gneissic to migmatitic *ca.* 3262–3245 Ma Maggo Gneiss. Crosscutting relationships and new geochronology data indicate that there are newly recognized volcanosedimentary sequences that are older than *ca.* 3262 and 3124 Ma. The period between 3141–3105 Ma involved magmatism and the deposition of the HRG at *ca.* 3105 Ma. Whether the volcanosedimentary sequence older than *ca.* 3124 Ma is part of a previously undocumented older phase of the HRG remains to be tested. Subsequently, the intrusion of a plutonic suite and the deposition of the FLG occurred between *ca.* 3032–2953 Ma. All of these rocks were intruded at *ca.* 2892–2832 Ma by the KIS; the youngest phases of the suite were synchronous with a regional metamorphic event from *ca.* 2846–2796 Ma. This was followed by synchronous plutonic and metamorphic events from *ca.* 2732–2700 Ma. The youngest recorded Archean event is the intrusion of the *ca.* 2578–2545 Ma alkaline Aucoin Plutonic suite and a locally preserved *ca.* 2554–2542 Ma metamorphism.

Linking the thermal and plutonic record to demonstrated tectonic events in the Archean rocks of the Hopedale Block remains elusive. Locally the Maggo Gneiss and *ca.* 3107 Ma orthogneisses preserve evidence of a cryptic metamorphism at *ca.* 2961–2953 Ma (zircon overgrowths in two samples). Most metaplutonic rocks preserve evidence of widespread metamorphism during the intervals *ca.* 2846–2796 Ma (zircon overgrowth and titanite growth) and *ca.* 2732–2700 Ma (zircon overgrowth and titanite growth). The *ca.* 2846–2796 Ma metamorphic event is geographically widespread and synchronous, in part, with the intrusion of the KIS. It is herein suggested that the KIS represents a continental magmatic arc that formed during the initiation of modern-style, subduction-driven, plate tectonics in the region. The *ca.* 2732–2700 Ma metamorphic event likely corresponds to the collision between the Saglek and Hopedale blocks. The *ca.* 2554–2542 Ma event is thus far only documented locally and may be restricted to the western Hopedale Block. To further refine the metamorphic history in the region, detailed geochronology of the deformation fabrics coupled with P-T data is required.

ACKNOWLEDGMENTS

Fieldwork was supported by colleagues at the GSC (Roger Paulen and Jessey Rice) and at the GSNL (Heather Campbell), all of whom contributed immensely to the success of this project. Student assistant Amelia Kennedy is thanked for her tireless efforts during fieldwork. Fieldwork also benefitted from the knowledge of Aqvituk (Hopedale) community members Shavonne Tuglavina, Allan Pijogge, Albert Tuglavina, Edmund Saunders, and Patty Dicker. We are grateful for the support and assistance of the staff of the Geochronology Laboratories of the Geological Survey of Canada. In particular, Ray Chung, Greg Case and Tom Pestaj are thanked for their careful efforts and excellent work. Matt Polivchuk provided the necessary high-quality zircon SEM images. This research was conducted in part on Labrador Inuit Lands with permission of the Nunatsiavut Government, NGRAC-19577773. This is Natural Resources Canada Contribution number 20230426. The manuscript was improved by the helpful reviews of John Hinchey. Kim Morgan is thanked for cartographic support.

REFERENCES

Barton Jr., J.M.
1975: The Mugford Group Volcanics of Labrador: Age, geochemistry, and tectonic setting. Canadian Journal of Earth Sciences, Volume 12, pages 1196-1208. https://doi.org/10.1139/e75-109

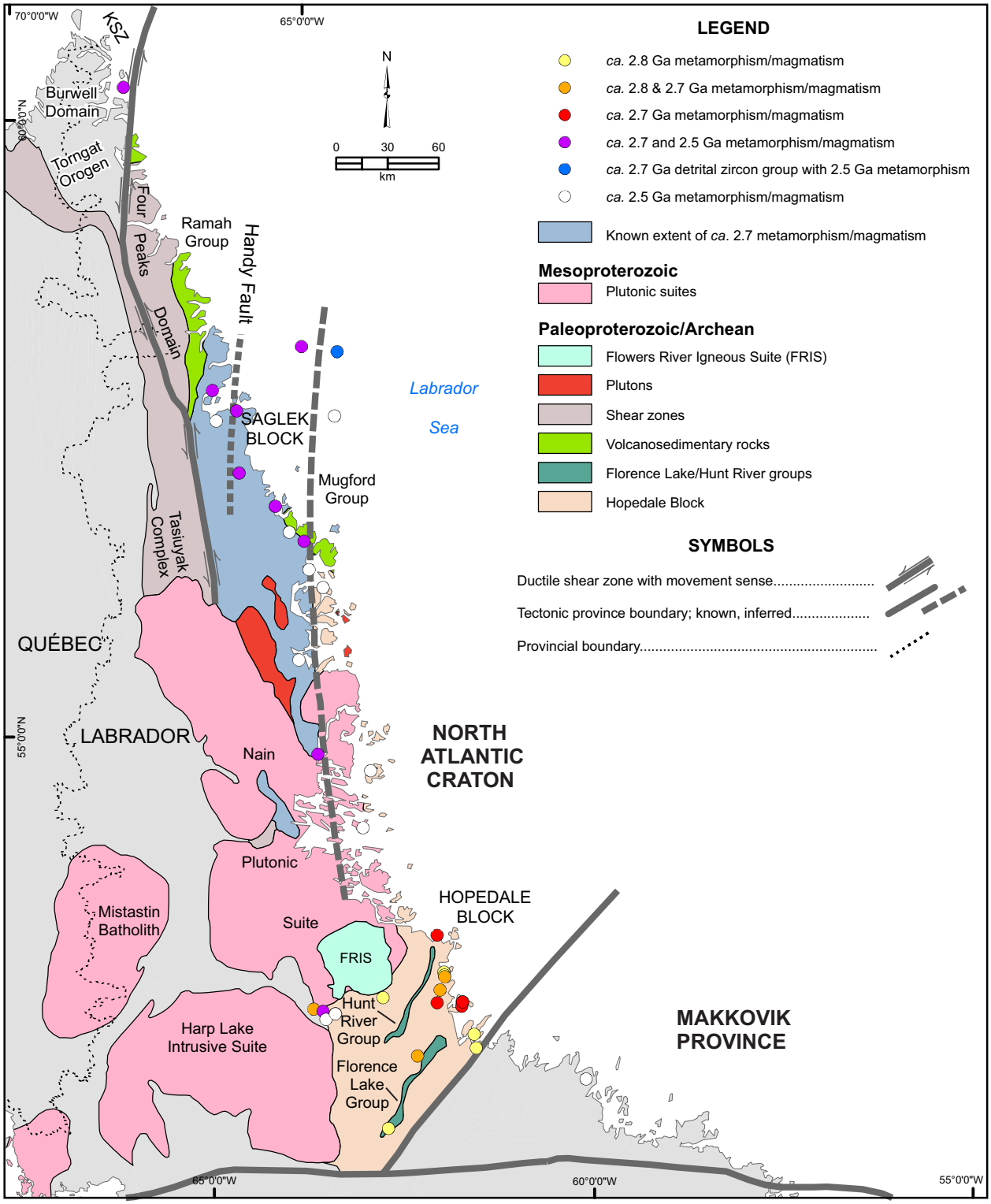

Figure 6. *Simplified tectonic setting of the North Atlantic Craton in Labrador illustrating the extent of 2.7 and 2.5 Ga metamorphism. Saglek data based on published works (*see *Wanless* et al.*, 1970, 1974; Barton Jr., 1975; Schiøtte* et al.*, 1989, 1990; Scott, 1995; Wasteneys* et al.*, 1996; Connelly and Ryan, 1999; Connelly, 2001; Krogh and Kamo, 2006; Kusiak* et al.*, 2018; Sałacińska* et al.*, 2018). Source data for the Hopedale Block is referenced in Table 1. The boundary between the Saglek and Hopedale blocks, originally proposed by Connelly and Ryan (1996) was slightly modified after Dunkley* et al. *(2019).*

Bodorkos, S., Bowring, J.F. and Rayner, N.M.
2020: Squid3: Next-generation data processing software for sensitive high-resolution ion microprobe (SHRIMP). https://doi.org/10.11636/133870

Bridgewater, D., Watson, J.V. and Windley, B.F.
1973: A discussion on the evolution of the Precambrian crust - the Archaean craton of the North Atlantic region. Philosophical Transactions of the Royal Society of London, Series A, Mathematical and Physical Sciences, Volume 273, pages 493-512. https://doi.org/10.1098/rsta.1973.0014

Cadman, A.C., Heaman, L., Tarney, J., Wardle, R. and Krogh, T.E.
1993: U–Pb geochronology and geochemical variation within two Proterozoic mafic dyke swarms, Labrador. Canadian Journal of Earth Sciences, Volume 30, pages 1490-1504. https://doi.org/10.1139/e93-128

Connelly, J.N.
2001: Constraining the timing of metamorphism: U-Pb and Sm-Nd Ages from a Transect across the Northern Torngat Orogen, Labrador, Canada. The Journal of Geology, Volume 109, pages 57-77. https://doi.org/10.1086/317965

Connelly, J.N. and Ryan, A.B.
1996: Late Archean evolution of the Nain Province, Nain, Labrador: Imprint of a collision. Canadian Journal of Earth Sciences, Volume 33, pages 1325-1342. https://doi.org/10.1139/e96-100

1999: Age and tectonic implications of Paleoproterozoic granitoid intrusions within the Nain Province near Nain, Labrador. Canadian Journal of Earth Sciences, Volume 36, pages 833-853. https://doi.org/10.1139/e99-002

Davis, W.J., Pestaj, T., Rayner, N. and McNicoll, V.M.
2019: Long-term reproducibility of $^{207}Pb/^{206}Pb$ age at the GSC SHRIMP lab based on the GSC Archean reference zircon z1242. https://doi.org/10.4095/321203

Diekrup, D., Hinchey, A.M., Campbell, H.E., Rayner, N. and Piercey, S.J.
2023: Stratigraphy, structure, and mineral potential of the 3.0 Ga Florence Lake greenstone belt, Labrador. *In* Current Research. Government of Newfoundland and Labrador, Department of Industry, Energy and Technology, Geological Survey, Report 23-1, pages 151-161.

Ducharme, T.A.
2018: Petrogenesis, Emplacement Setting, and Magmatic-hydrothermal Mineralization of the peralkaline Flowers River Igneous Suite, Hopedale Block, Labrador. M.Sc. thesis, The University of New Brunswick, 156 pages.

Dunkley, D.J., Kusiak, M.A., Wilde, S.A., Whitehouse, M.J., Sałacińska, A., Kielman, R. and Konečný, P.
2019: Two neoarchean tectonothermal events on the western edge of the North Atlantic craton, as revealed by SIMS dating of the Saglek Block, Nain Province, Labrador. Journal of the Geological Society, Volume 177, pages 31-49. https://doi.org/10.1144/jgs2018-153

Ermanovics, I.
1980: Geology of the Hopedale Block of Nain Province, Labrador; Report 2, Nain-Makkovik Boundary Zone. In Current Research, Part B. Geological Survey of Canada, Paper 80-1B, pages 11-15. https://doi.org/10.4095/102146

1993: Geology of Hopedale Block, southern Nain Province, and the adjacent Proterozoic terranes, Labrador, Newfoundland. Geological Survey of Canada, Volume 431, pages 1-161. https://doi.org/10.4095/183986

Feely, M., Wilton, D.H., Costanzo, A., Kollar, A.D., Goudie, D.J. and Joyce, A.
2019: Mineral Liberation Analysis and Scanning Electron Microscopy of Connemara Marble: New mineral distribution maps of an iconic Irish gem material. The Journal of Gemmology, Volume 36, pages 456-466. https://doi.org/10.15506/JoG.2019.36.5.456

Godet, A., Guilmette, C., Labrousse, L., Smit, M.A., Cutts, J.A., Davis, D.W. and Vanier, M.
2021: Lu–Hf garnet dating and the timing of collisions: Palaeoproterozoic accretionary tectonics revealed in the Southeastern Churchill Province, Trans-Hudson Orogen, Canada. Journal of Metamorphic Geology, Volume 39, pages 977-1007. https://doi.org/10.1111/jmg.12599

Hill, J.D.
1991: Emplacement and tectonic implications of the mid-Proterozoic peralkaline Flowers River Igneous Suite, north-central Labrador. Precambrian Research, Volume 49, pages 217-227. https://doi.org/10.1016/0301-9268(91)90033-7

Hinchey, A.M., Diekrup, D. and Rayner, N.
2023a: Revisiting Mesoproterozoic magmatism in Labrador: Evaluating AMCG and peralkaline magmatism. *In* Current Research. Government of Newfoundland and Labrador, Department of Industry, Energy and Technology, Geological Survey, Report 23-1, pages 181-196.

Hinchey, A.M., Rayner, N. and Davis, W.J.
2020: Episodic Paleoproterozoic crustal growth preserved in the Aillik Domain, Makkovik Province, Labrador. Precambrian Research, Volume 337. https://doi.org/10.1016/j.precamres.2019.105526

Hinchey, A.M., Sandeman, H.A. and Butler, J.P.
2023b: The Paleoproterozoic granite factory: Voluminous post-collisional, ferroan, A-type granites and implications for crust formation and metallogenic tenor, Labrador, Canada. Geological Society of America Bulletin. https://doi.org/10.1130/B36727.1

James, D.T.
1997: The Archean Hunt River Greenstone Belt, Hopedale Block, eastern Labrador (NTS 13N/7 and 13N/10): Geology and exploration potential. *In* Current Research. Government of Newfoundland and Labrador, Department of Mines and Energy, Geological Survey, Report 97-1, pages 9-27.

James, D.T., Kamo, S. and Krogh, T.
2002: Evolution of 3.1 and 3.0 Ga volcanic belts and a new thermotectonic model for the Hopedale Block, North Atlantic craton (Canada). Canadian Journal of Earth Sciences, Volume 39, pages 687-710. https://doi.org/10.1139/e01-092

Ketchum, J.W.F., Culshaw, N.G. and Barr, S.M.
2002: Anatomy and orogenic history of a Paleoproterozoic accretionary belt: The Makkovik Province, Labrador, Canada. Canadian Journal of Earth Sciences, Volume 39, pages 711-730. https://doi.org/10.1139/e01-099

Korstgård, J. and Ermanovics, I.
1985: Tectonic evolution of the Archean Hopedale block and the adjacent Makkovik Subprovince, Labrador, Newfoundland. *In* Evolution of Archean Supracrustal Sequences. *Edited by* L.D. Ayres, P.C/ Thurston, K.D. Card and W. Weber. Geological Association of Canada, Special Paper 28, pages 223-237.

Krogh, T.E. and Kamo, S.L.
2006: Precise U-Pb zircon ID-TIMS ages provide an alternative interpretation to early ion microprobe ages and new insights into Archean crustal processes, northern Labrador. *In* Processes on the Early Earth. Geological Society of America. https://doi.org/10.1130/2006.2405(06)

Kusiak, M.A., Dunkley, D.J., Whitehouse, M.J., Wilde, S.A., Sałacińska, A., Konečný, P., Szopa, K., Gawęda, A. and Chew, D.
2018: Peak to post-peak thermal history of the Saglek Block of Labrador: A multiphase and multi-instrumental approach to geochronology. Chemical Geology, Volume 484, pages 210-223. https://doi.org/10.1016/j.chemgeo.2017.10.033

Loveridge, W., Ermanovics, I.F. and Sullivan Loverid, R.W.
1987: U-Pb ages on zircon from the Maggo Gneiss, the Kanairiktok Plutonic Suite and the Island Harbour Plutonic Suite, coast of Labrador, Newfoundland. *In* Radiogenic Age and Isotopic Studies. Geological Survey of Canada, Report 1, pages 59-65.

Ludwig, K.
2009: SQUID 2: A User's Manual. Berkeley Geochronology Center Special Publication, Berkeley, Volume 2, 104 pages.

2012: Users manual for Isoplot/Ex: A geochronological toolkit for Microsoft Excel. Berkeley Geochronology Center, Berkeley, Special Publication 5, 110 pages.

Rayner, N.M.
2022: Report on U-Pb geochronology from the 2017-2020 GEM-2 activity "Saglek Block, Labrador: Geological evolution and mineral potential". Geological Survey of Canada, Open File 8901, 17 pages. https://doi.org/10.4095/330237

Sahin, T. and Hamilton, M.A.
2019: New U-Pb baddeleyite ages for Neoarchean and Paleoproterozoic mafic dyke swarms of the southern Nain Province, Labrador: Implications for possible plate reconstructions involving the North Atlantic craton. Precambrian Research, Volume 329, pages 44-69. https://doi.org/10.1016/j.precamres.2019.02.001

Sałacińska, A., Kusiak, M.A., Whitehouse, M.J., Dunkley, D.J., Wilde, S.A. and Kielman, R.
2018: Complexity of the early Archean Uivak Gneiss: Insights from Tigigakyuk Inlet, Saglek Block, Labrador, Canada and possible correlations with south West Greenland. Precambrian Research, Volume 315, pages 103-119. https://doi.org/10.1016/j.precamres.2018.07.011

Sandeman, H.A.I., Hinchey, A.M., Diekrup, D. and Campbell, H.E.
2023: Lithogeochemical and Nd isotopic data for Hunt River Belt and Weekes amphibolite, Hopedale Block, Labrador: Evidence for two stages of mafic magmatism at >3200 and ~3100 Ma. *In* Current Research. Government of Newfoundland and Labrador, Department of Industry, Energy and Technology, Geological Survey, Report 231, pages 7798.

Sandeman, H.A.I. and McNicoll, V.J.
2015: Age and petrochemistry of rocks from the Aucoin gold prospect (NTS map area 13N/6), Hopedale Block, Labrador: Late Archean, alkali monzodiorite–syenite hosts Proterozoic orogenic Au–Ag–Te mineralization. *In* Current Research. Government of Newfoundland and Labrador, Department of Natural Resources, Geological Survey, Report 15-1, pages 85-103.

Schiøtte, L., Compston, W. and Bridgwater, D.
1989: U–Th–Pb ages of single zircons in Archaean supracrustals from Nain Province, Labrador, Canada. Canadian Journal of Earth Sciences, Volume 26, pages 2636-2644. https://doi.org/10.1139/e89-224

Schiøtte, L., Noble, S. and Bridgwater, D.
1990: U-Pb mineral ages from northern Labrador: Possible evidence for interlayering of Early and Middle Archean tectonic slices. Geoscience Canada. https://journals.lib.unb.ca/index.php/GC/article/view/3693 (accessed January 2024).

Scott, D.J.
1995: U–Pb geochronology of the Nain craton on the eastern margin of the Torngat Orogen, Labrador. Canadian Journal of Earth Sciences, Volume 32, pages 1859-1869. https://doi.org/10.1139/e95-143

Steiger, R.H. and Jäger, E.
1977: Subcommission on geochronology: Convention on the use of decay constants in geo- and cosmochronology. Earth and Planetary Science Letters, Volume 36, pages 359-362. https://doi.org/10.1016/0012-821X(77)90060-7

Stern, R.A.
1997: The GSC Sensitive High Resolution Ion Microprobe (SHRIMP): analytical techniques of zircon U-Th-Pb age determinations and performance evaluation. *In* Radiogenic Age and Isotopic Studies: Report 10. Geological Survey of Canada, Current Research 1997-F, pages 1-31. https://doi.org/10.4095/209089

Stern, R.A., and Amelin, Y.
2003: Assessment of errors in SIMS zircon U–Pb geochronology using a natural zircon standard and NIST SRM 610 glass. Chemical Geology, Volume 197, pages 111-142. https://doi.org/10.1016/S0009-2541(02)00320-0

Wanless, R.K., Stevens, R.D., Lachance, G.R. and Delabio, R.N.
1970: Age determinations and geological studies, K-Ar isotopic ages, Report 9. Geological Survey of Canada, Paper 69-2A, 78 pages. https://doi.org/10.4095/102305

1974: Age determinations and geological studies K-Ar Isotopic ages, report 12. Geological Survey of Canada, Paper 74-2, 78 pages. https://doi.org/10.4095/102880

Wardle, R.
1993: Geology of the Naskaupi River Region, Central Labrador (13 NW). Government of Newfoundland and Labrador, Department of Mines and Energy, Geological Survey Branch, Map 93-16, Scale 1:500 000.

Wardle, R.J., James, D.T., Scott, D.J. and Hall, J.
2002: The southeastern Churchill Province: Synthesis of a Paleoproterozoic transpressional orogen. Canadian Journal of Earth Sciences, Volume 39, pages 639-663. https://doi.org/10.1139/e02-004

Wasteneys, H., Wardle, R.J., Krogh, T., Ermanovics, I. and Hall, J.
1996: U-Pb geochronological constraints on the deposition of the Ingrid Group and implications for the Saglek - Hopedale and Nain Craton - Torngat Orogen Boundaries. Eastern Canadian Shield Onshore-Offshore Transect (ECSOOT), Report of the 1996 Transect Meeting. Compiled by R.J. Wardle and J. Hall. Lithoprobe Report, Volume 57, pages 212-228.